Investigation of the Relationship between HIC and Impact Conditions in Scooter-type Powered-Two-Wheeler-to-Car Crashes

Toshiyuki Yanaoka, Yasuaki Gunji, Zarir Hafiz Zulkipli, Tetsuya Matsushita, Jolyon Carroll, Pradeep Puthan, Siti Atiqah Mohd Faudzi, Kak D-Wing, Yusuke Miyazaki

Abstract Understanding impact mechanisms is essential for reducing fatalities in Powered-Two-Wheeler (PTW) crashes. This study examined how impact parameters (velocities, angle and location) and helmet-fastening condition influenced the Head Injury Criterion (HIC15) across various PTW-to-Car crash conditions, with the aim of identifying representative conditions for a passive safety performance evaluation method. A total of 5,088 PTW-front to car-side impact simulations were analysed using the finite element models of six production cars and two scooter-type PTWs, and a motorcyclist dummy, to clarify the relationship between HIC15 and impact parameters. The results showed that helmet-fastening condition and knee kinematics following knee impact with the car significantly influenced HIC15. In addition, perpendicular impact to the pillars tended to produce high HIC15 values regardless of impact speed and angle. Based on this large number of simulations, three main findings were obtained for scooter-type PTW-to-Car impacts: (1) a database which can be used for the analysis for not only head but also other injuries was established; (2) the results suggest the need for careful consideration of the helmet-fastening condition when designing a testing method; and (3) high HIC15 values were consistently observed in perpendicular impacts, indicating that this configuration may be a candidate for representative impact condition.

Keywords Passive safety, PTW-to-Car crash, FE simulation database, HIC, Impact conditions

I. INTRODUCTION

As reported by the Global Status Report on Road Safety 2023 [1], Powered-Two-Wheeler (PTW) riders account for around 30% of all road traffic deaths worldwide, rising to 46% in Southeast Asia. These statistics show that reducing the death toll among PTW riders, especially in Southeast Asia, is critical for achieving the target of a considerable reduction in road traffic deaths throughout the world.

Various efforts and research activities have been undertaken around the world to reduce fatalities among PTW riders. These include measures to mitigate or reduce the impact speed in traffic accidents (e.g. education [2-3], mandatory installation of anti-lock brake systems [4], and investigating the introduction of Advanced Rider Assistance Systems (ARAS) [5]). In addition to these activities and investigations, technology for reducing the severity of injury for a given impact (passive safety technology) has been investigated, and PTWs have been equipped with such technologies (e.g. airbags) [6-9].

In parallel with the progress of passive safety technologies, evaluation methods for quantifying performance of personal protective equipment have been developed (e.g. methods for limb joint protectors [10], back protectors [11], chest protectors [12], inflatable protectors [13], protective garments [14] and methods using PTW-to-Car tests and simulations [15]). However, there is no simple evaluation method for PTW safety performance in PTW-to-Car impacts representing real-world fatal accident.

The ultimate goal of this study is to develop a simple method that can evaluate PTW passive safety performance comparable to existing test methods for car passive safety. To achieve this goal, investigations have been carried out to identify: (1) the target crash configuration (e.g. PTW-front to car-side); (2) impact conditions appropriate for the evaluation of passive safety performance; (3) an appropriate testing method; and (4) suitable evaluation

T. Yanaoka (e-mail: toshiyuki_yanaoka@jp.honda; tel: +81-80-3212-7581) is Assistant Chief Engineer at Honda R&D Co., Ltd. Japan and a PhD student in system engineering at the Institute of Science Tokyo. Y. Gunji is Chief Engineer at Honda R&D Co., Ltd. Z. H. Zulkipli is VRU head at the Malaysian Institute of Road Safety Research (MIROS). T. Matsushita is Key Account Manager at Autoliv Japan Inc. J. Carroll is senior researcher at Autoliv Development AB. P. Puthan is researcher at Autoliv Asia ROH Co., Ltd. S. A. Mohd Faudzi and K. D-Wing are researchers at MIROS. Y. Miyazaki is Associate Professor at the Institute of Science Tokyo.

criteria. As part of this effort, Zulkipli *et al.* [16] analysed Malaysian crash data and identified the PTW-front to car-side impact as a priority crash configuration. In addition, according to the accident data, fatalities due to head injury account for 37 to 56% in number of fatalities of PTW riders [17-18], suggesting the importance of reducing the head injury probability. Although rotational motion of the head causes strain in the brain due to its incompressible nature, Head Injury Criterion [19] (HIC15) has a certain relationship with brain strain [20] possibly due to existence of a certain relationship between brain strain and kinetic energy of the head before impact. Based on these facts, as a first step towards method development, Yanaoka *et al.* [21] analysed the influence of impact condition on whole-body trajectories in PTW-to-Car impacts and found that the rider's head moved approximately in-plane until impact with the car. Based on this finding, Yanaoka *et al*. [22] investigated the relationship between Head Injury Criterion (HIC15) and impact parameters, including head impact location on the car, using six combinations of production cars and a production PTW, and applied the knowledge from the earlier study to efficiently conduct a large number of simulations. Although that study [22] clarified the relationship between HIC15 and key impact parameters, two issues remained: (1) the effect of another PTW type commonly found in the Southeast Asian market, namely the flat-floor scooter-type; and (2) the influence of partial helmet removal motion before the head impact.

This study aimed to examine how the head impact location, impact angle, car velocity, PTW velocity, and partial helmet removal influences the HIC15 across various PTW-to-Car crash combinations, thereby providing fundamental insights for identifying crash conditions appropriate for the evaluation of passive safety.

II. METHODS

In this study, PTW-front to car-side simulations were conducted by changing not only the impact conditions but also the combination of car and PTW, thereby clarifying the relationship between impact conditions and HIC15 and how HIC15 is affected when the combination of car and PTW is changed. The influence of the helmet fitting to the PTW driver's head was also investigated. Overall, the methodology is the same as that used in [26], which allows us to compare the results under the same initial impact conditions. The TSUBAME 4.0 supercomputer at the Institute of Science Tokyo was used for all the simulations performed in this study.

Simulation Models

The simulation models used in this study consisted of six production car models, two production PTW models and one anthropometric test device (ATD) model as a rider. All simulation models used in this study were finite element (FE) models.

Car Models: six production car models – K-car, compact, small sedan, middle sedan, SUV and mini-van – were used to represent the diversity of the cars available on the market. The car model used in this study was the same as the models used in [26]. All car models were developed in the same manner to represent technical drawings of the production car model and validated against the in-house experiment for pole side impact test condition defined in UN Regulation No. 135 [23] in terms of local deformation and global motion of the car. To accurately simulate the post-crash dynamics, the tyres, the wheels, and the handlebars were modelled to closely represent the actual car. Major specifications (length, width, height, weight, and number of elements) are shown in Table I. Figure 1 shows the car models used in this study.

TABLE I
SPECIFICATIONS OF THE CAR MODELS

	Length (mm)	Width (mm)	Height (mm)	Weight (kg)	No. of Elements (million)		Length (mm)	Width (mm)	Height (mm)	Weight (kg)	No. of Elements (million)
Car1	3395	1475	1545	900	6.8	Car4	4800	1750	1840	1840	8.4
Car2	3995	1695	1540	1260	3.8	Car5	4975	1860	1450	1580	9.1
Car3	4560	1800	1415	1490	2.2	Car6	4605	1855	1680	1590	5.7

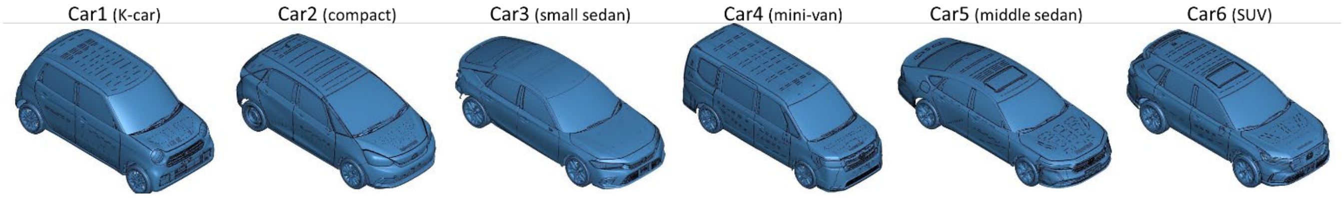

Fig. 1. Six car models.

PTW Models: the PTW models used in this study are a step-through scooter-type PTW and a flat-floor scooter-type PTW, because these types of PTW are commonly used in Southeast Asian countries. The addition of the flat-floor scooter-type in this study, adopted from [22], was intended to capture a common Southeast Asian PTW architecture in which rider posture and lower-limb interaction with the vehicle may differ from those of the step-through scooter-type. The step-through scooter-type PTW is the same as that used in [22]. The FE models were developed from the drawings of a production PTW model and validated against the in-house crash experiment for full-flat rigid barrier at 50 km/h in terms of local deformation and global motion of the vehicle. This model includes all major components. All components, except for the engine, were modelled as deformable, since deformation of the PTW is expected to influence the trajectory of the PTW rider. Furthermore, the tyres, wheels, and handlebar were modelled to rotate in a manner consistent with the actual PTW kinematics, since the rotation of the tyre and the handlebar are expected to influence the in-crash kinematics of the PTW driver. Each model consists of approximately 200,000 elements. Figure 2 shows the FE models of the PTWs used in this study.

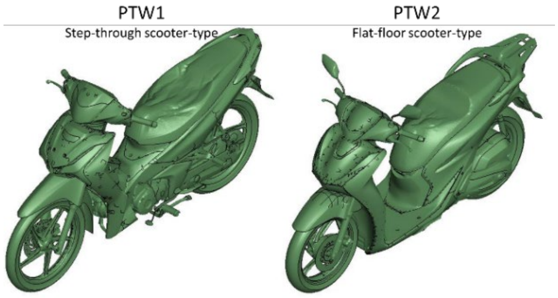

Fig. 2. PTW models

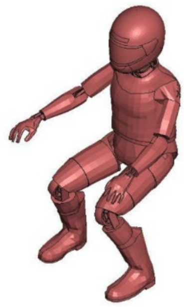

Fig. 3. MATD model.

Occupant model: for this study, the Motorcyclist Anthropometric Test Device (MATD) with helmet was used as the driver, as this dummy is the only one that meets all of the requirements defined in ISO 13232 [15]. The FE model of the MATD with helmet was the same as that used in [22] and its kinematics and kinetics against the PTW front to car side perpendicular impact at 50 km/h were validated previously [7]. This model consists of deformable parts and 200,000 elements. Based on the findings from the study by Yanaoka *et al.* [22], this study investigated the sensitivity of HIC15 to helmet-head coupling. Representing conditions in which the rider either normally fastened or tightly fastened the helmet, two contact conditions were defined between the MATD head and the inner surface of the helmet: sliding contact for the condition identified in the validation scheme with friction coefficient of 0.4 (normally fastened) and tied contact (tightly fastened). These conditions were used as boundary-condition extremes to represent different levels of relative motion between the head and the helmet, rather than as direct reproductions of specific real-world helmet-fastening states. The MATD model is shown in Fig. 3.

Output

To investigate the relationship between impact conditions, helmet fitting condition, and HIC15, output data were extracted from all simulations for both rider kinematics and structural deformation. Head motion was evaluated using the translational and rotational accelerations at the centre of gravity of the head, corresponding to its six-degree-of-freedom response. In parallel, the time history of deformation for the entire model was examined to capture the overall crash sequence, including rider trajectory, contact behaviour, and local deformation of the interacting structures. These outputs provided the basis for assessing the mechanisms of head impact and for clarifying the influence of impact parameters and helmet fitting condition on HIC15.

Impact Conditions

The impact conditions were characterised by four key parameters (Head Impact Target, Impact Angle, PTW Velocity, and Car Velocity), which were the same as Yanaoka *et al.* [22]. The definitions of these four parameters, along with the axis system, were consistent with those prescribed in [22] and are illustrated in Fig. 4. The impact parameter "Head Impact Target" was determined based on the findings from [21]. To adequately account for the diversity of possible impact scenarios and to ensure adequate coverage of structurally rigid zones (e.g. car pillars), three steps were specified in combinations for all PTW–car simulation scenarios (details are described in [22]).

1. Identification of structurally stiff locations.
2. Identification of tendency with PTW speed change.
3. Identification of the effect of change of the impact parameters around and between the pillars of a car.

A total of 212 simulations were conducted for each of the 24 combinations of six cars, two PTWs, and two types of contact setting between the head and the helmet inner. Six combinations of cars and step-through scooter-type with sliding contact were analysed in the study conducted by [22], that means a total of 3,816 full-FE PTW-to-Car impact simulations were additionally conducted. (A total of 5,088 simulation results were used in this study.)

Influential factor to HIC15

A multiple regression model was developed to analyze the effect of various parameters on HIC15. Categorical variables were encoded using dummy variables, and the contribution of each parameter was quantified using an incremental R^2 approach. Specifically, each factor was removed from the full model to evaluate the reduction in R^2, which represents its contribution to the total variance in HIC15. This method is equivalent to a regression-based ANOVA and allows for consistent comparison of both numerical and categorical variables.

Normalisation of Head Impact Location

The location values were transferred in the following manner in order to normalise by the location of the pillars, allowing comparison between the cars (using the same method as [22]).

- Coordinate values of Head Impact Targets in the longitudinal direction of the car were defined for A-pillar, B-pillar, and C-pillar as 0, 0.5, and 1, respectively.
- Coordinates of Head Impact Targets not located on pillars were calculated from linear interpolation and extrapolation by using the normalised coordinates of A-pillar, B-pillar, and C-pillar (e.g. the coordinate of the halfway point between the A-pillar and the B-pillar is 0.25).

A schematic of the normalised Head Impact Location is shown in Fig. 4.

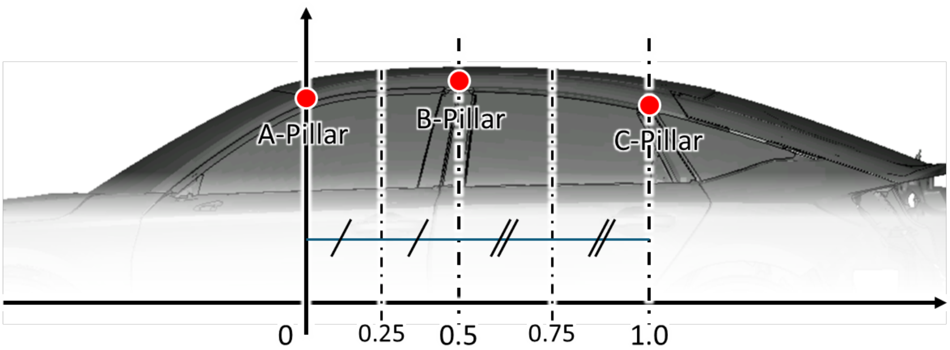

Fig. 4. Schematic of normalised Head Impact Target.

III. RESULTS

HIC15 values for each of the impact conditions were calculated from a total of 5,088 FE simulation results (212 simulations for each of the 24 combinations of car, PTW and contact settings). The results are shown for each of the steps in order to determine the combination of the impact parameters. In addition, the comparison of contribution of each parameter to variation of HIC15 is also shown in this section.

Results are presented in four parts: the effect of head impact target; the effect of PTW velocity; the combined effect of impact angle and vehicle speeds at representative pillar locations; and the variation in HIC15 associated with the helmet–head contact condition.

Average, standard deviation, minimum and maximum values of HIC15 are shown in Table AI

Change of Head Impact Target

Figure 5 shows the HIC15 value distribution by Head Impact Target for each of the six cars (K-car, compact, small sedan, mini-van, middle sedan, SUV).

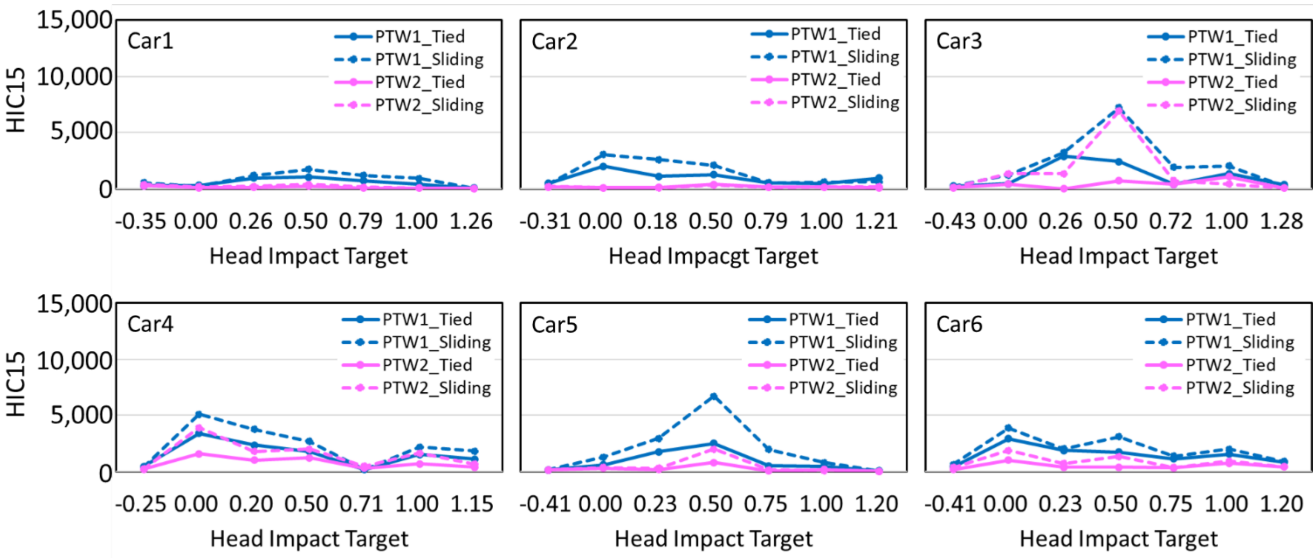

Fig. 5. HIC15 value distribution by Head Impact Target for Car1 to Car6.

Across all vehicle classes, HIC15 tended to be elevated at pillar locations, with B-pillar impacts showing particularly high values in Cars 1, 3, and 5, while Cars 2, 4, and 6 showed elevated responses across multiple pillar locations. In addition, HIC15 was generally lower for PTW2 than for PTW1, and lower under tied helmet–head contact than under sliding contact.

Change of PTW Velocity

HIC15 value distributions by Head Impact Target for each PTW velocity are shown in Figs. 6–11. The coordinates of the Head Impact Target were normalised in the same manner as described in the previous section.

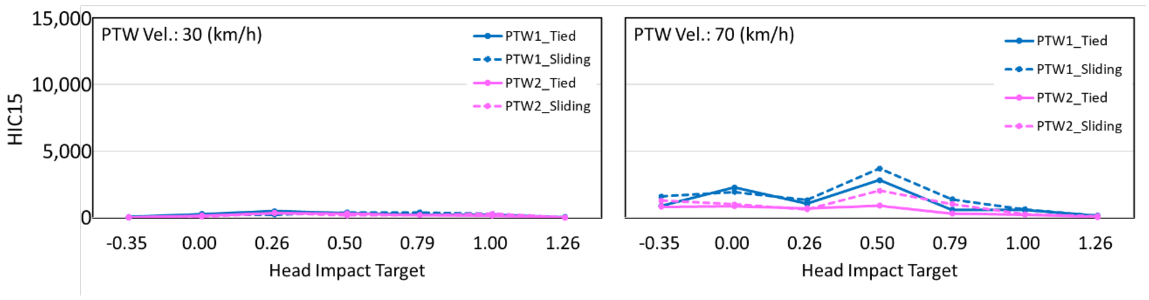

Fig. 6. HIC15 value distribution by Head Impact Target for Car1 (PTW velocity: 30 and 70 km/h).

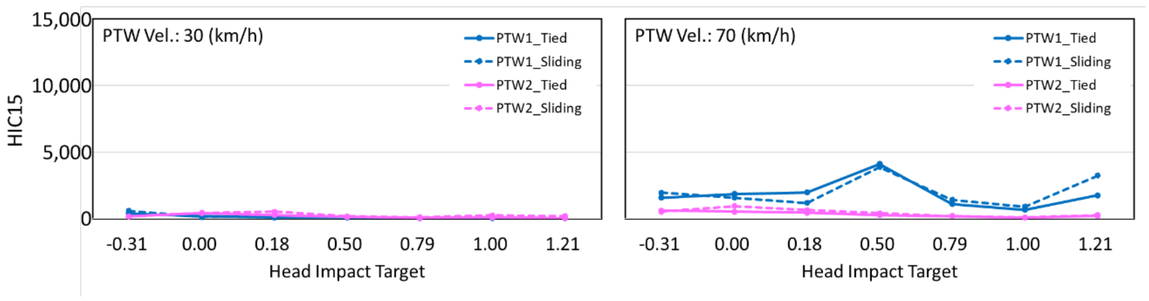

Fig. 7. HIC15 value distribution by Head Impact Target for Car2 (PTW velocity: 30 and 70 km/h).

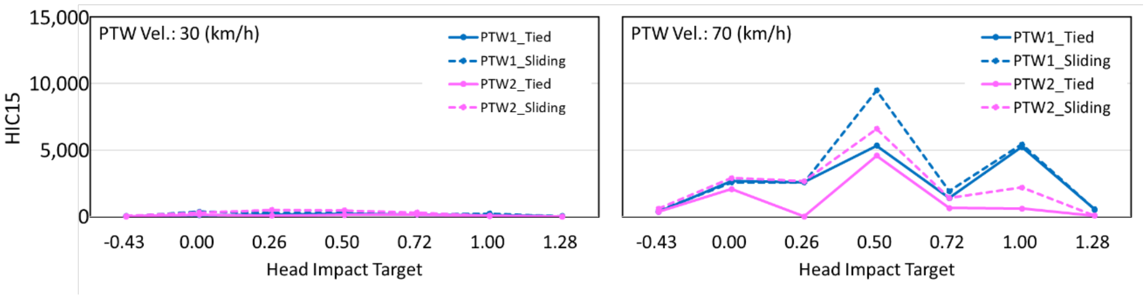

Fig. 8. HIC15 value distribution by Head Impact Target for Car3 (PTW velocity: 30 and 70 km/h).

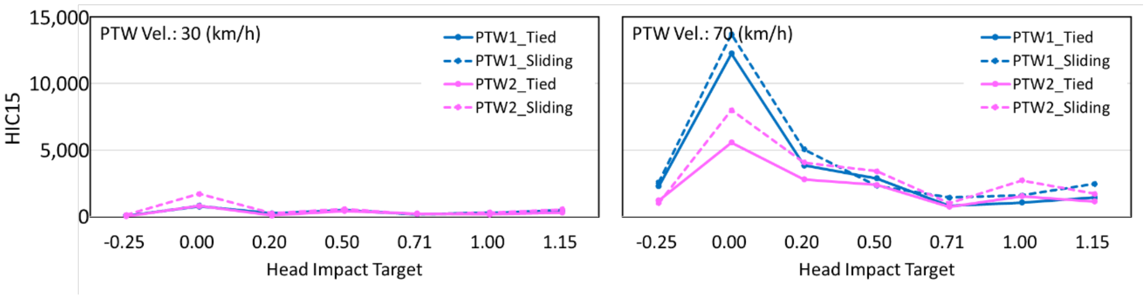

Fig. 9. HIC15 value distribution by Head Impact Target for Car4 (PTW velocity: 30 and 70 km/h).

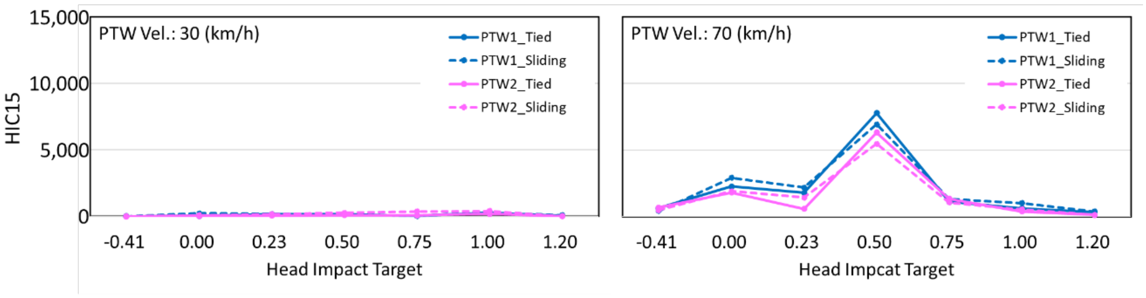

Fig. 10. HIC15 value distribution by Head Impact Target for Car5 (PTW velocity: 30 and 70 km/h).

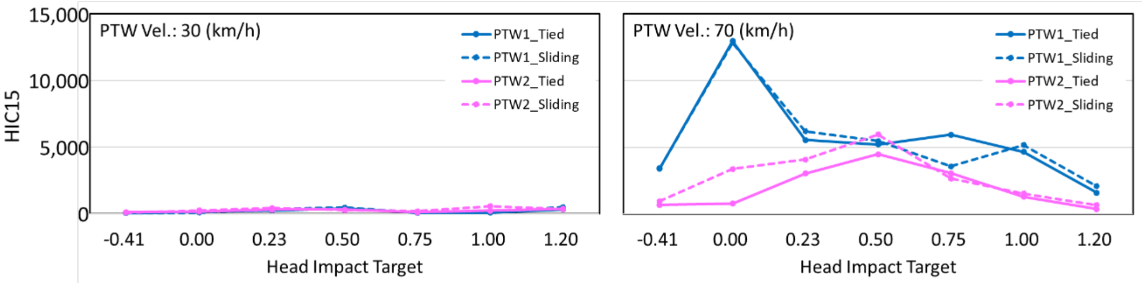

Fig. 11. HIC15 value distribution by Head Impact Target for Car6 (PTW velocity: 30 and 70 km/h).

From the comparison of the results shown in Figs. 5 and Figs. 6–11, the following observations were made. There are two tendencies, regardless of the Car type: (1) HIC15 values in PTW2 impact were smaller than those in PTW1; and (2) HIC15 values decreased when the contact condition between the head and helmet inner was changed from sliding to tied.

For Car1, Car3, and Car5, the tendency for the B-pillar to produce higher HIC15 values than the other head impact locations at a PTW velocity of 50 km/h remained unchanged when the PTW velocity was varied to 30 km/h or 70 km/h. In contrast, for Car4 and Car6, HIC15 values at the A-pillar increased when the PTW velocity was raised to 70 km/h. For Car2, the HIC15 value at the B-pillar increased, resulting in a trend similar to that observed for Car1, Car3, and Car5.

Change of Impact Angle, Car Velocity, and PTW Velocity

Figures 12–20 show examples of the relationship between HIC15 and three impact parameters (Impact Angle, Car velocity, and PTW velocity) for each of the pillars (Car6 for A-pillar and B-pillar, and Car1 for C-pillar). All graphs for each of six cars' results are shown in Figs. B1–B3, C1-C3, D1-D3, E1-E3, F1-F3 and G1-G3 in the Appendix.

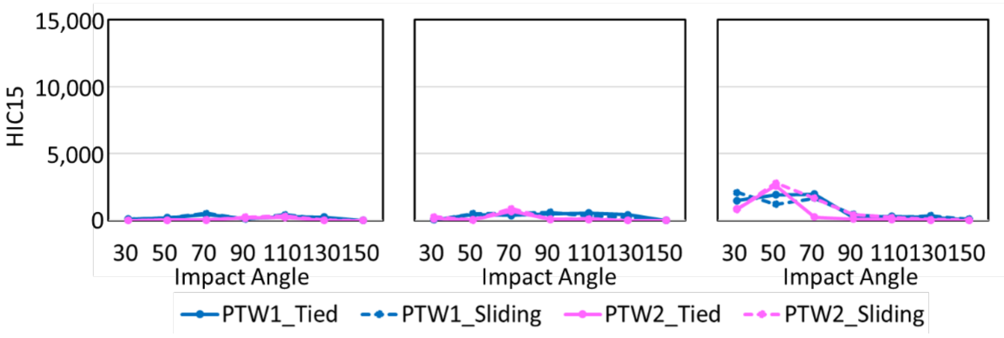

Fig. 12. Relationship between HIC15, and impact angle and car velocity (PTW velocity: 30 km/h, Car6, A-pillar).

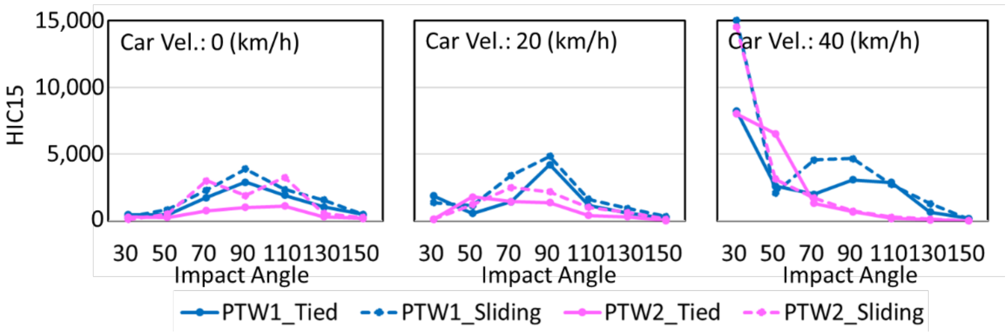

Fig. 13. Relationship between HIC15, and impact angle and car velocity (PTW velocity: 50 km/h, Car6, A-pillar).

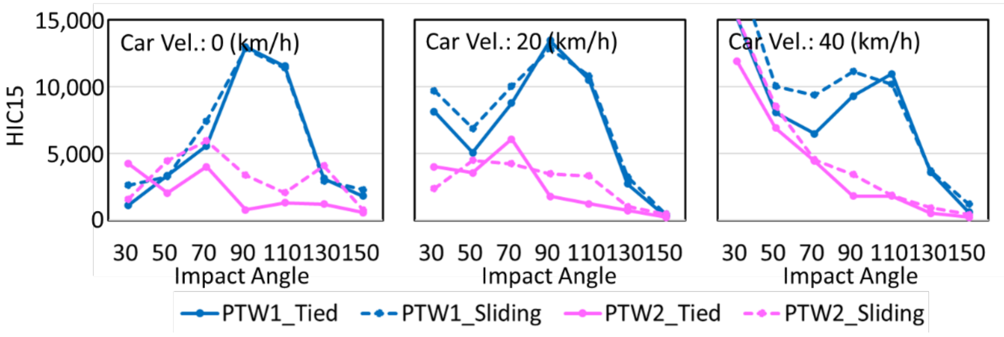

Fig. 14. Relationship between HIC15, and impact angle and car velocity (PTW velocity: 70 km/h, Car6, A-pillar).

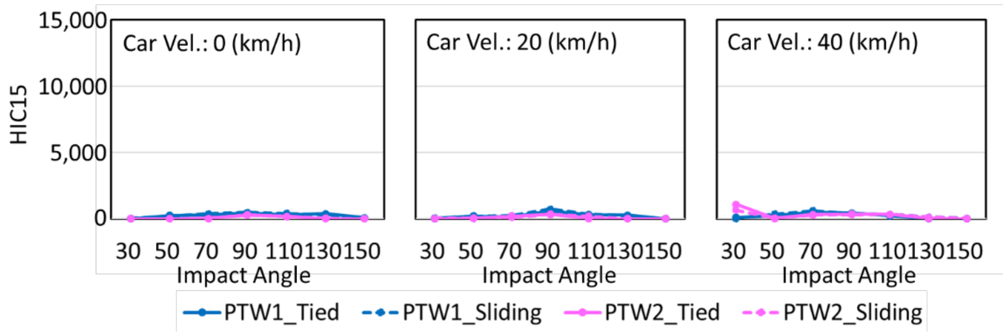

Fig. 15. Relationship between HIC15, and impact angle and car velocity (PTW velocity: 30 km/h, Car6, B-pillar).

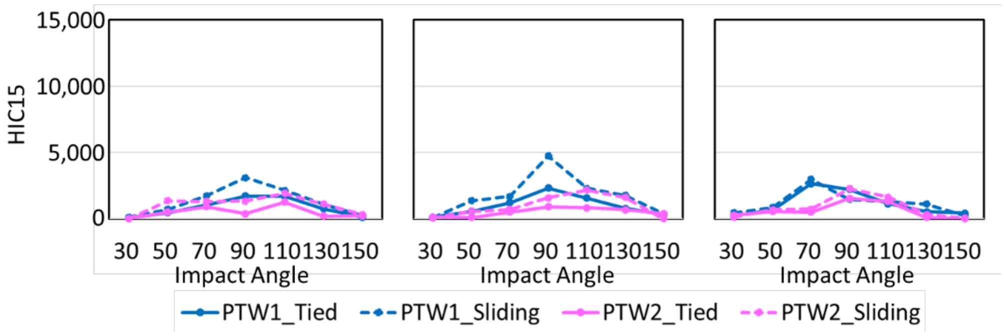

Fig. 16. Relationship between HIC15, and impact angle and car velocity (PTW velocity: 50 km/h, Car6, B-pillar).

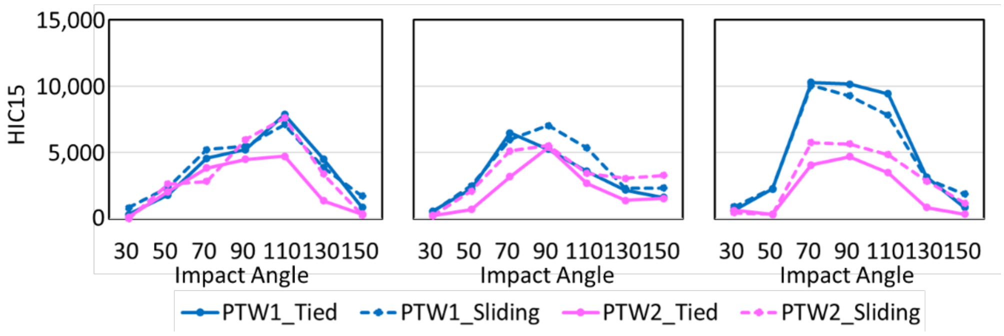

Fig. 17. Relationship between HIC15, and impact angle and car velocity (PTW velocity: 70 km/h, Car6, B-pillar).

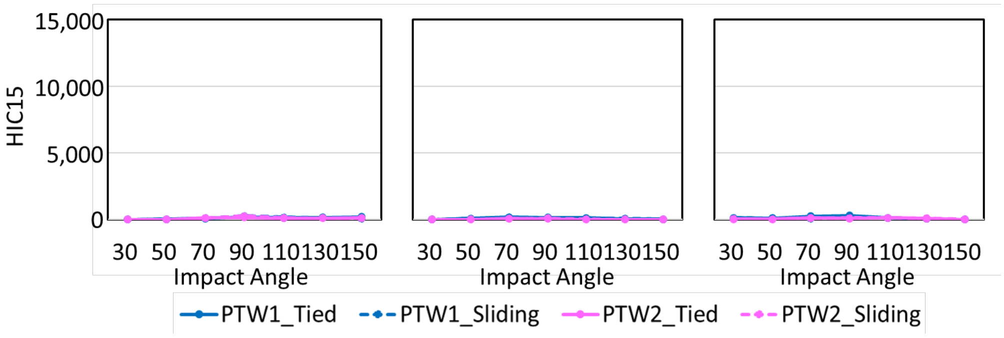

Fig. 18. Relationship between HIC15, and impact angle and car velocity (PTW velocity: 30 km/h, Car1, C-pillar).

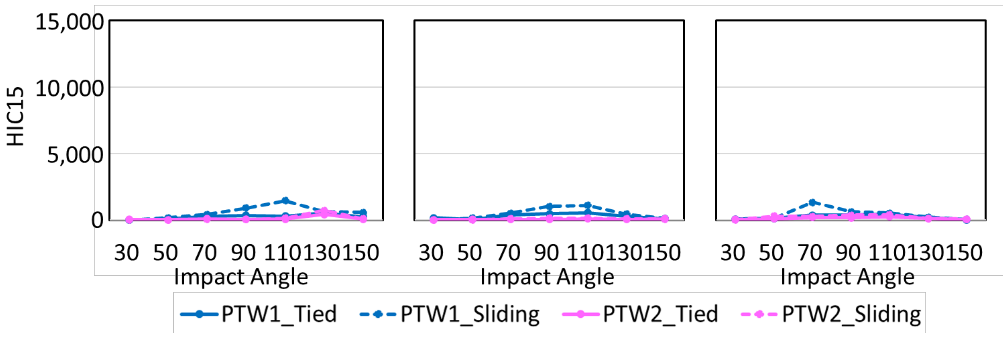

Fig. 19. Relationship between HIC15, and impact angle and car velocity (PTW velocity: 50 km/h, Car1, C-pillar).

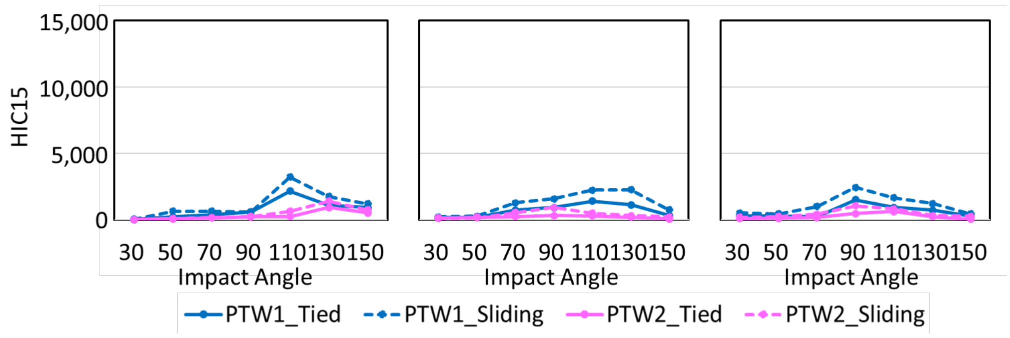

Fig. 20. Relationship between HIC15, and impact angle and car velocity (PTW velocity: 70 km/h, Car1, C-pillar).

Following on from Figs. 12–20, the following tendencies were found in A-pillar impact:

- HIC15 increased when the impact angle was close to 90°;
- HIC15 increased with decrease of impact angle and increase of Car velocity.

In addition, for B-pillar, when the impact angle was close to 90°, maximum HIC15 value was observed.

Furthermore, in C-pillar impact, the opposite tendency to the A-pillar was observed, i.e. HIC15 increased with increase of impact angle and decrease of Car velocity.

Influential factor to HIC15

Contribution ratio (ratio of variation by each parameter to total variation) to HIC15 is shown in Fig. 21.

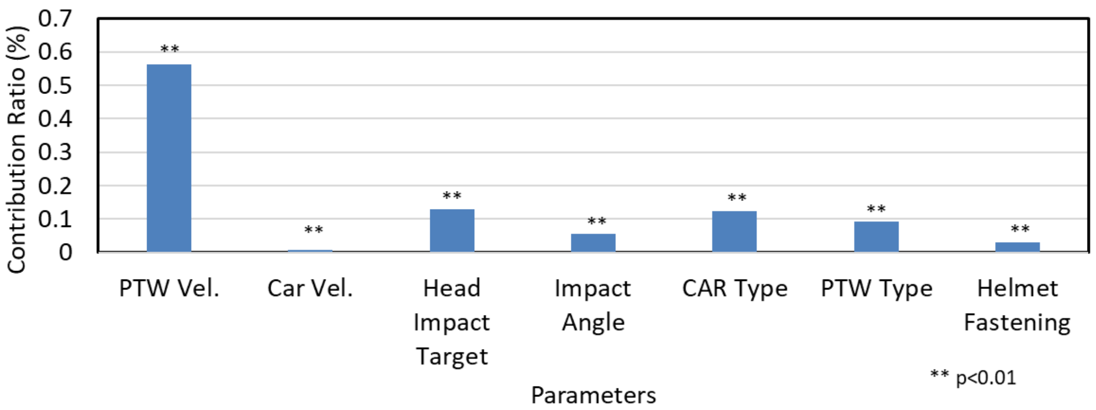

Fig. 21. Contribution ratio of each parameters to HIC15 variation

From Fig. 26, it is found that the contribution ratio of PTW velocity, Car velocity and other parameters are 0.56, 0.008 and 0.03 to 0.13, respectively.

IV. DISCUSSION

From Table AI, the maximum value of HIC15 in this study exceeds 30,000. Although the maximum value of HIC15 indicates high probability of AIS6 (over 90 %), this result is comparable with the HIC15 value in the car to pedestrian impact simulation conducted by Takahashi et al. [24] when considering the inclusion of the impact condition in which the chin of MATD directly impacts to the pillars due to partial helmet removal.

As can be seen in Figs. 5–11, HIC15 values generally decreased when the contact condition between the head and the helmet inner was changed from sliding contact to tied contact. Table AI also shows that the S.D. of HIC15 value also decreased under the tied contact condition. This is consistent with the occurrence of partial helmet removal in some conditions. These findings suggest that the partial helmet removal motion observed in [22] was avoided when the helmet was tightly constrained to the head. This suggests that helmet fastening is a critical factor when considering the repeatability and reproducibility of a future performance evaluation test. However, while the kinematics of the MATD and helmet were validated against the PTW-to-car impact [7] in a sliding contact condition (normal fastening condition), the tied contact condition was a parametric study to clarify the influence of removal motion during impact on HIC15. Further clarification on the influence of strength of fastening on HIC15 values may be needed in support of a test protocol for a performance evaluation test.

The distribution of HIC15 values also shows a general tendency for higher HIC15 to occur at pillar locations. This likely reflects differences in local structural stiffness along the roof-rail. As the roof-rail is supported by three or four pillars to maintain roof strength and preserve occupant survival space during rollover, the stiffness at the pillar-supported regions is expected to be higher than at other locations. As a result, impacts to these regions are more likely to produce elevated HIC15 values.

Comparison of the HIC15 distributions between PTW1 (step-through scooter-type) and PTW2 (flat-floor scooter-type) (refer to Figs. 5–25) shows that HIC15 values were generally lower in PTW2 impacts than PTW1 impacts. Figure 27 shows the posture of the MATD at the time of head impact. The extension angle of knee of MATD in PTW2 tended to be larger than that in PTW1. To clarify the difference of the posture, Fig. 28 compares the dummy posture at the time of knee impact. This comparison shows a difference in knee motion during and after contact with the car. In PTW1, the knee tended to move outward without sticking, allowing the extension angle of knee to be approximately 90 deg. until head impact. On the other hand, knee restriction was observed in PTW2, which caused the extension of knee after knee impact. Since the results of the FE simulation are deterministic, these differences in impact kinematics should be considered carefully during the design of testing methods to ensure adequate repeatability and reproducibility.

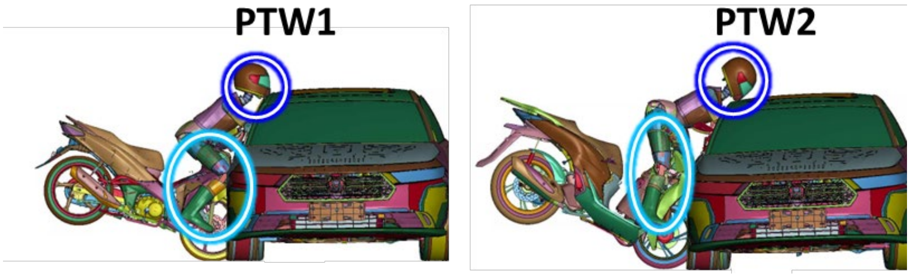

Fig. 27. Comparison of posture of MATD at the head impact between PTW1 and PTW2 for Car5 impact (PTW velocity: 50 km/h, Impact Angle: 90 deg. and Head Impact Location: 0.5).

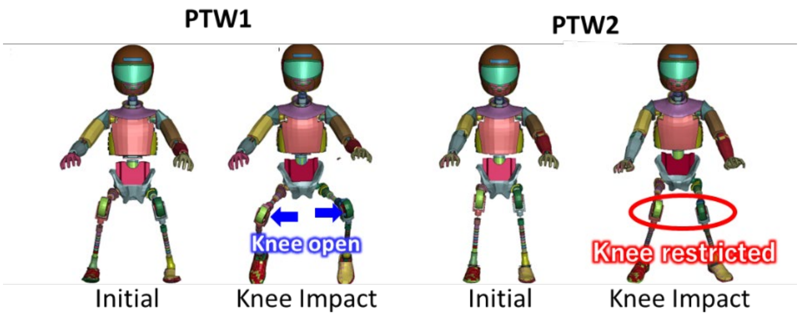

Fig. 28. Comparison of posture of MATD at the knee impact between PTW1 and PTW2 for Car5 impact (PTW velocity: 50 km/h, Impact Angle: 90 deg. and Head Impact Location: 0.5).

In terms of the influence of impact parameters (Impact angle, Car velocity and PTW velocity), different relationships with HIC15 were observed at pillar locations, except for high HIC15 in perpendicular impacts (approximately 90°), which was particularly seen at the B-pillar. At the A-pillar, HIC15 values in small angle impact (30° or 40°) increased with Car and PTW velocities compared with those in larger-angle impact (90° or greater). This appears to be a characteristic feature of A-pillar impacts. Since the A-pillar is located at the corner of the roof-rail, both PTW velocity and car velocity would become a component of relative velocity in line with the direction of reaction force from the car body to the head. This may explain the observed relationship between HIC15 and impact parameters.

For B-pillar impact, perpendicular impacts (approximately 90°) produced the highest HIC15 values regardless of PTW and Car velocities. In addition, Car velocity had only limited influence on HIC15 when the Car speed was 70 km/h. Unlike the A-pillar, the B-pillar does not form a corner-shaped geometry. This suggests that the reaction force from the car was caused only perpendicular to the roof-rail, and subsequently high HIC15 was observed only when the impact angle was near the perpendicular (this could be a possible reason for high HIC15 in perpendicular impact regardless of the Head Impact Location).

For the C-pillar impacts, the relationship between HIC15 and impact parameters displays an opposite tendency to that of A-pillar impacts. In general, HIC15 decreases with increase of impact angle (large impact angle, over 135°) and with decrease of car velocity. The C-pillar is the most rear-side pillar in some cars (e.g. Car1, Car2, Car3 and Car5). In these cars, C-pillar can be a corner when the impact angle is greater than 135°. Similar to the A-pillar case, both PTW velocity and car velocity may contribute to the component of relative velocity aligned with the direction of the reaction force. This could explain the general characteristics of the relationship between HIC15 and impact parameters.

In this study, over 5,000 simulation results were analysed to clarify the relationship between HIC15 and impact parameters. The findings, including the detailed results presented in the Appendix, provide an important basis for identifying impact conditions suitable for PTW crash safety performance evaluation. Although this study focused only on HIC15, given the importance of head injury in PTW fatalities, other injury metrics available from the MATD can also be derived from the same simulations. This suggests that the large amount of simulation data developed in this study may serve as a valuable foundation not only for head injury assessment, but also for evaluating injury risk in other body regions. Although this study focused on only HIC15, rotational motion of the head which causes brain strain should be investigated in future steps since the brain injury, which induces loss of metabolic activity in brain cells or hematoma in sub-dural space leading to an increase in intracranial pressure, can also result in a high risk of fatality.

Finally, this study used the FE model of the MATD, which is the only dummy that satisfies the requirements defined in ISO 13232 [15] (geometrical data, and component responses in quasi-static and dynamic condition). However, the kinematics of MATD in PTW-to-Car impacts has not been validated against experiments using postmortem human surrogates. Over the past two decades, FE Human Body Models (HBMs) have been developed to improve understanding of injury biomechanics during impact. Although these HBMs have not yet been validated for PTW impact condition, further investigation using such models would be valuable once their applicability to PTW-to-Car impacts is confirmed and may help to further assess the validity of the findings observed in this study.

V. CONCLUSION

From over 5,000 PTW-to-Car FE simulation results, a comprehensive database was developed, which can be used to investigate the relationship between not only HIC15 but also other injury metrics in various body region and impact conditions. This study extended previous PTW-to-car impact simulations by including two scooter configurations and two helmet–head contact conditions.

The following conclusions were drawn regarding the head impact location, car velocity, impact angle, and partial helmet removal across various PTW-to-Car crash combinations. The results confirmed that HIC15 was consistently influenced by helmet–head coupling (fastening), PTW type, and impact location, with pillar impacts generally producing the highest HIC15 values. Car speed only influenced the small impact angle crashes involving the A- or C-pillars; the perpendicular impact represents a worst-case scenario, regardless of the impact conditions selected. Therefore, among the impact locations assessed, near-perpendicular pillar impacts emerged as the primary candidate conditions for a future PTW passive safety evaluation, although further work is needed to examine additional injury criteria and model biofidelity.

PTW2 impacts tended to produce lower HIC15 than PTW1 impacts, likely due to differences in rider posture associated with lower-limb interaction during the impact sequence. As such, the HIC15 value may be significantly affected by the helmet-fastening condition and knee interactions. This suggests the necessity of careful consideration of both rider posture and helmet fastening-and-retention when working on a test method for such an impact.

VI. ACKNOWLEDGEMENTS

The TSUBAME 4.0 supercomputer at the Institute of Science Tokyo was used in this study. Approximately 15 million core*hours were needed to finish all of the FE simulations. The authors would like to express their great appreciation for the high performance, flexibility, and applicability of TSUBAME 4.0, which enabled the authors to efficiently complete a large number of simulations in such a short period.

VII. REFERENCES

[1] World Health Organization (2023) Global status report on road safety 2023.
[2] Suzuka Circuit Traffic Education Center, Honda Mobilityland, https://www.suzukacircuit.jp/eng/stec/bike/school/assays/, accessed 15 January 2026.
[3] International Motorcycle Manufacturers Association (2010) Motorcycle Safety: IMMA's contribution to the Decade of Action for Road Safety 2011-20.
[4] Hamzah, A. (2023) Adoption of vehicle safety regulations in Malaysia. High-Level 15th Regional Environmentally Sustainable Transport Forum in Asia, Kuala Lumpur, Malaysia.
[5] Kaye, S. A., *et. al*. (2024) Exploring beliefs and perceptions towards Advanced Rider Assistance Systems (ARAS) in motorcycle safety. *Transportation Research Part F: Traffic Psychology and Behavior*, **102**: pp. 77–87.
[6] Rogers N. M. and Zellner, J. W. (2001) Factors and status of motorcycle airbag feasibility research. *Proceedings of the 17th International Technical Conference on the Enhanced Safety of Vehicles (ESV)*, Amsterdam, Paper No.01-S9-O-207.
[7] Kuroe, T., Namiki, H., Iijima, S. (2005) Exploratory study of an airbag concept for a large touring motorcycle: Further research second report. *Proceedings of the 19th International Technical Conference on the Enhanced Safety of Vehicles (ESV)*, Washington D.C., USA, Paper No. 05-0316.
[8] Bhosale, P. V. (2013) Exploratory study on the suitability of an airbag for Indian motorcycle using finite element computer simulations of rigid wall barrier tests. *Proceedings of the 23rd International Technical Conference on the Enhanced Safety of Vehicles (ESV)*, Seoul, Paper No. 13-0195.
[9] Aikyo, Y., Kobayashi, Y., Akashi, T., Ishiwatari, M. (2015) Feasibility Study of Airbag Concept Applicable to Motorcycles Without Sufficient Reaction Structure. *Traffic Injury Prevention*, **16**(sup1): pp. S148–S152. https://doi.org/10.1080/15389588.2015.1016156.
[10] European Committee for Standardization (2013) EN 1621-1:2013, Motorcyclists' protective clothing against mechanical impact - Part 1: Motorcyclists' limb joint impact protectors – requirements and test methods.
[11] European Committee for Standardization (2014) EN 1621-2:2014, Motorcyclists' protective clothing against mechanical impact - Part 2: Motorcyclists' back protectors – requirements and test methods.
[12] European Committee for Standardization (2019) EN 1621-3:2019, Motorcyclists' protective clothing against mechanical impact - Part 3: Motorcyclists' chest protectors – requirements and test methods.
[13] European Committee for Standardization (2013) EN 1621-4:2013, Motorcyclists' protective clothing against mechanical impact - Part 4: Motorcyclists' inflatable protectors – requirements and test methods.
[14] European Committee for Standardization (2020) EN 17092:2020, Protective garments for motorcycle riders
[15] International Organization for Standardization (2012) ISO 13232:2012, Motorcycles - Test and analysis procedures for research evaluation of rider crash protective devices fitted to motorcycles.
[16] Zulkipli, Z. H., *et. al*. (2025) Star rating for Safer Motorcycle in South East Asia – ASEAN MAP. International Conference on Safety and Holistic Intervention for Future Vehicles, Selangor, Malaysia.
[17] Pathak, H. M., Waghmare V. N., Tasgaokar, G. V. (2025) Type of injuries encountered in an autopsy based study of deaths due to motorcycle accidents at a tertiary care centre. *International Journal of Medicine and Public Health*, **15**(2)
[18] Japanese Government Statistics. Statistics about Road Traffic Annual Report Yearly 2025. https://www.e-stat.go.jp/en/stat-search/files?tclass=000001020602&cycle=7&year=20250, accessed 20 May 2026.
[19] Versace J. A. (1971) Review of the Severity Index. *Proceeding of the 15th Stapp Car Crash Conference*. pp.771-796.
[20] Takhounts E. G., Craig M. J., Moorhouse K., McFadden J., Hasija V. (2013) Development of brain injury criteria (BrIC). *Stapp Car Crash Journal*. 57:243-66.
[21] Yanaoka, T., Aikyo, Y., Gunji, Y. (2025) Investigation of Influence of Impact Condition on Whole Body Trajectory of Powered Two-Wheeler Driver in Collision to Car Side. *International Journal of Automotive Engineering*, **16**(4).
[22] Yanaoka, T., *et al*. (2026) A Study on the Relationship between Impact Conditions and Head Injury Criterion (HIC) in Powered-Two-Wheeler to Car Crashes. SAE Technical Paper 2026-01-0571.
[23] United Nations. (2016) Regulation No. 135: Uniform provisions concerning the approval of vehicles with regard to their Pole Side Impact performance (PSI).
[24] Takahashi, Y., Yanaoka, T., Sugaya, H., Basilio, A. V., Xu, P., Ateshian, G., & Morrison, B. (2019). Prediction of probability of fatality due to brain injury in traffic accidents. Traffic Injury Prevention, 20(sup1), S27–S31. https://doi.org/10.1080/15389588.2019.1591621

VIII. APPENDIX

Appendix A: Average, standard deviation, minimum and maximum values of HIC15

TABLE A1

AVERAGE, STANDARD DEVIATION, MINIMUM AND MAXIMUM VALUES OF HIC15

Car	Helmet Fastening (Contact Type)	Average	Standard Deviation	Maximum	Minimum
Car1	Normal (Sliding contact)	920	1523	12840	0
	Tight (Tied contact)	647	1089	8163	1
Car2	Normal (Sliding contact)	653	1020	8075	1
	Tight (Tied contact)	506	796	6759	1
Car3	Normal (Sliding contact)	2052	4017	33630	1
	Tight (Tied contact)	1173	2474	26010	0
Car4	Normal (Sliding contact)	1782	2495	15300	1
	Tight (Tied contact)	1373	2111	14640	0
Car5	Normal (Sliding contact)	1271	1841	14600	0
	Tight (Tied contact)	892	1415	9506	1
Car6	Normal (Sliding contact)	1748	2657	18850	0
	Tight (Tied contact)	1401	2284	15090	1

Appendix B: Influence of Impact Angle, Car Velocity and PTW Velocity (CAR1)

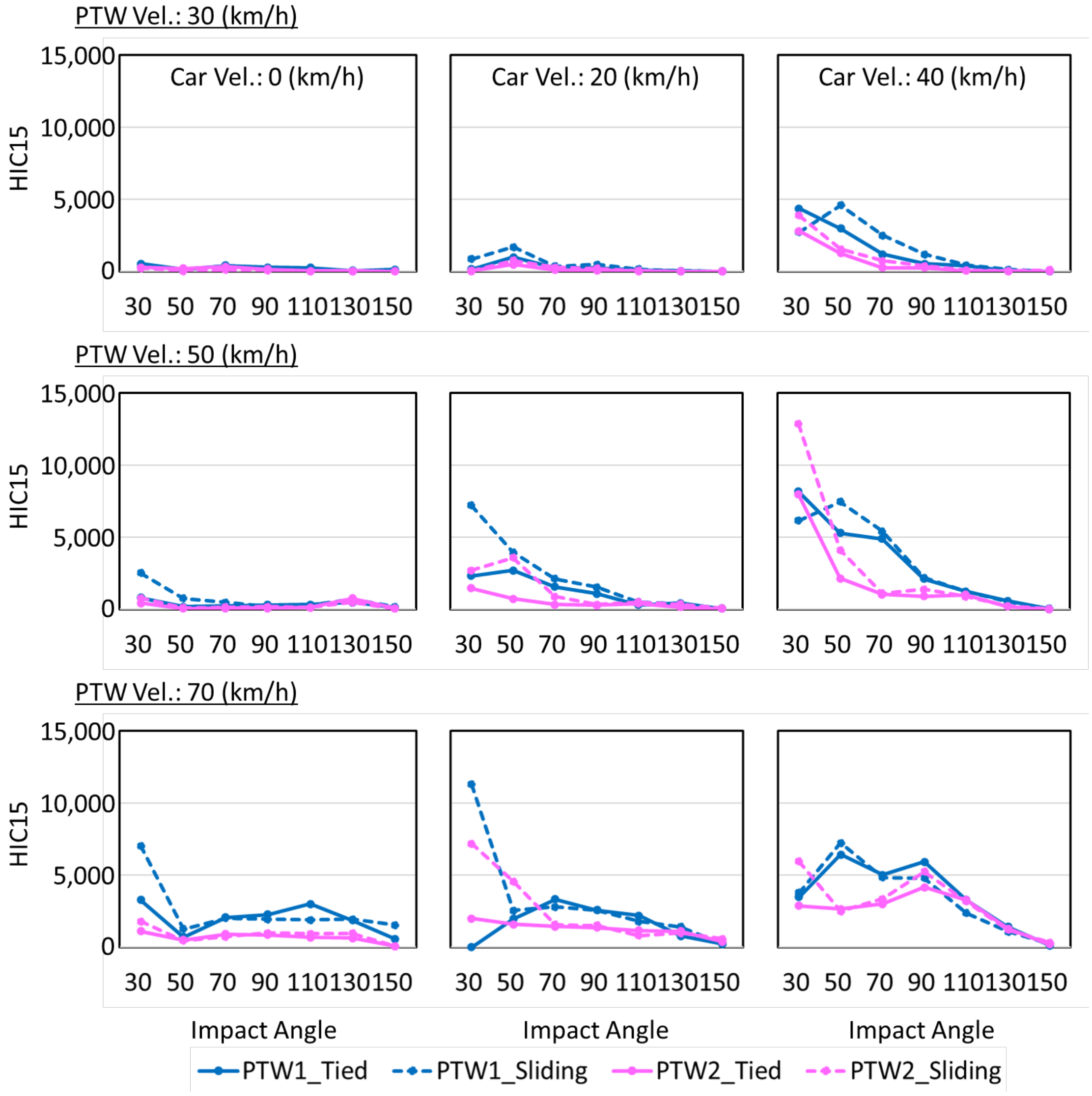

Fig. B1. Relationship between HIC15, and impact angle, car velocity and PTW velocity (A-pillar).

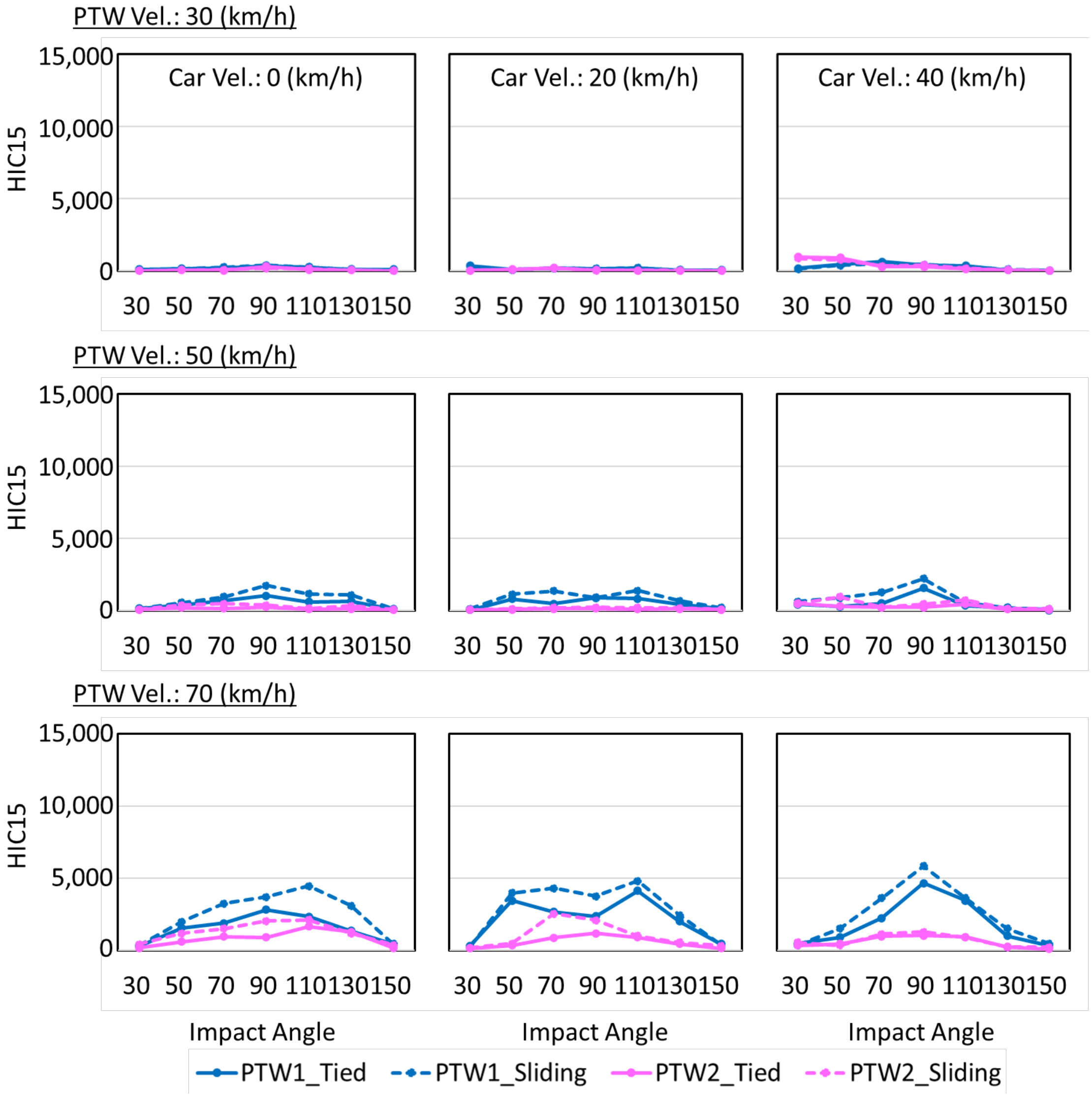

Fig. B2. Relationship between HIC15, and impact angle, car velocity and PTW velocity (B-pillar).

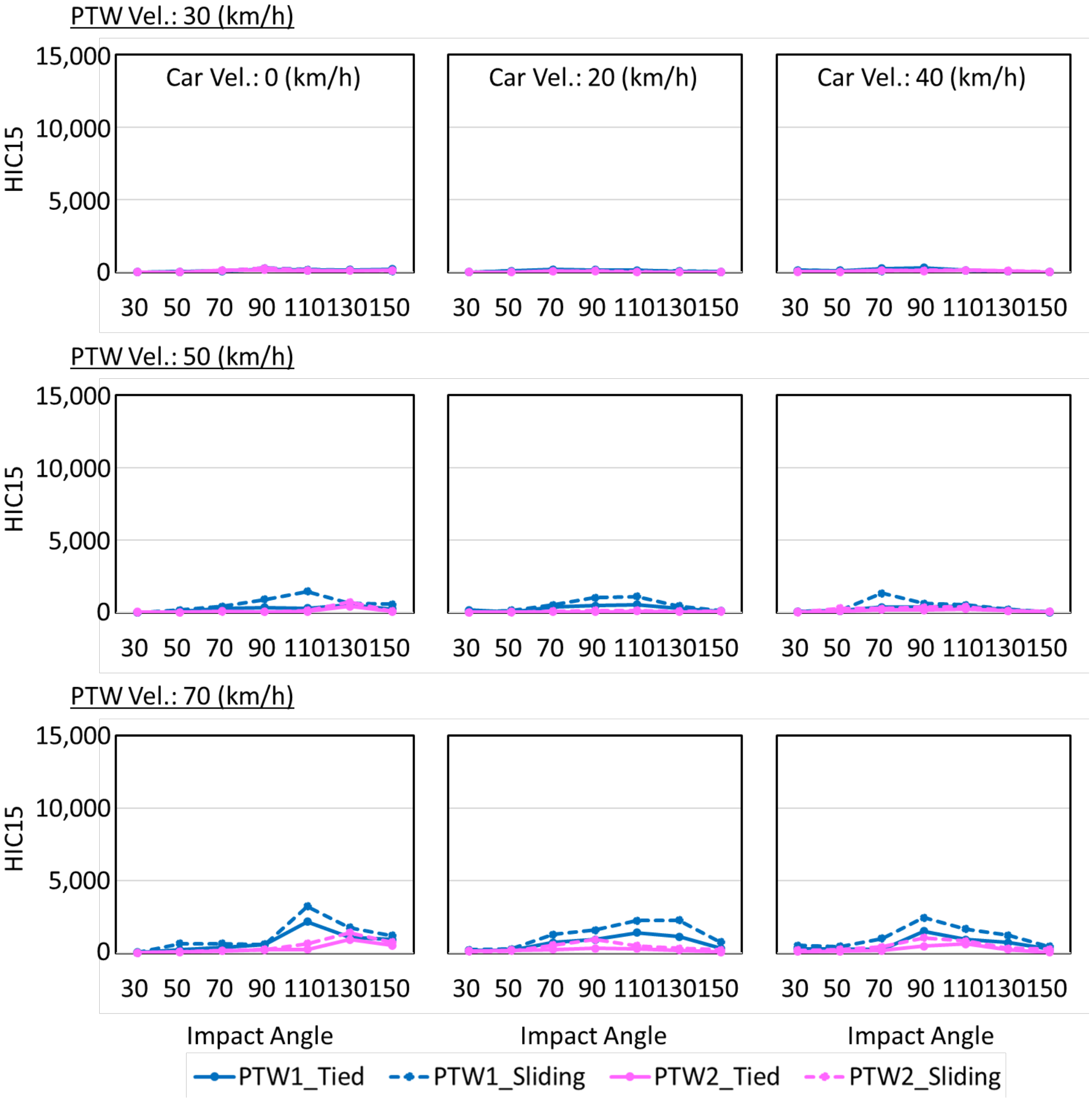

Fig. B3. Relationship between HIC15, and impact angle, car velocity and PTW velocity (C-pillar).

Appendix C: Influence of Impact Angle, Car Velocity and PTW Velocity (CAR2)

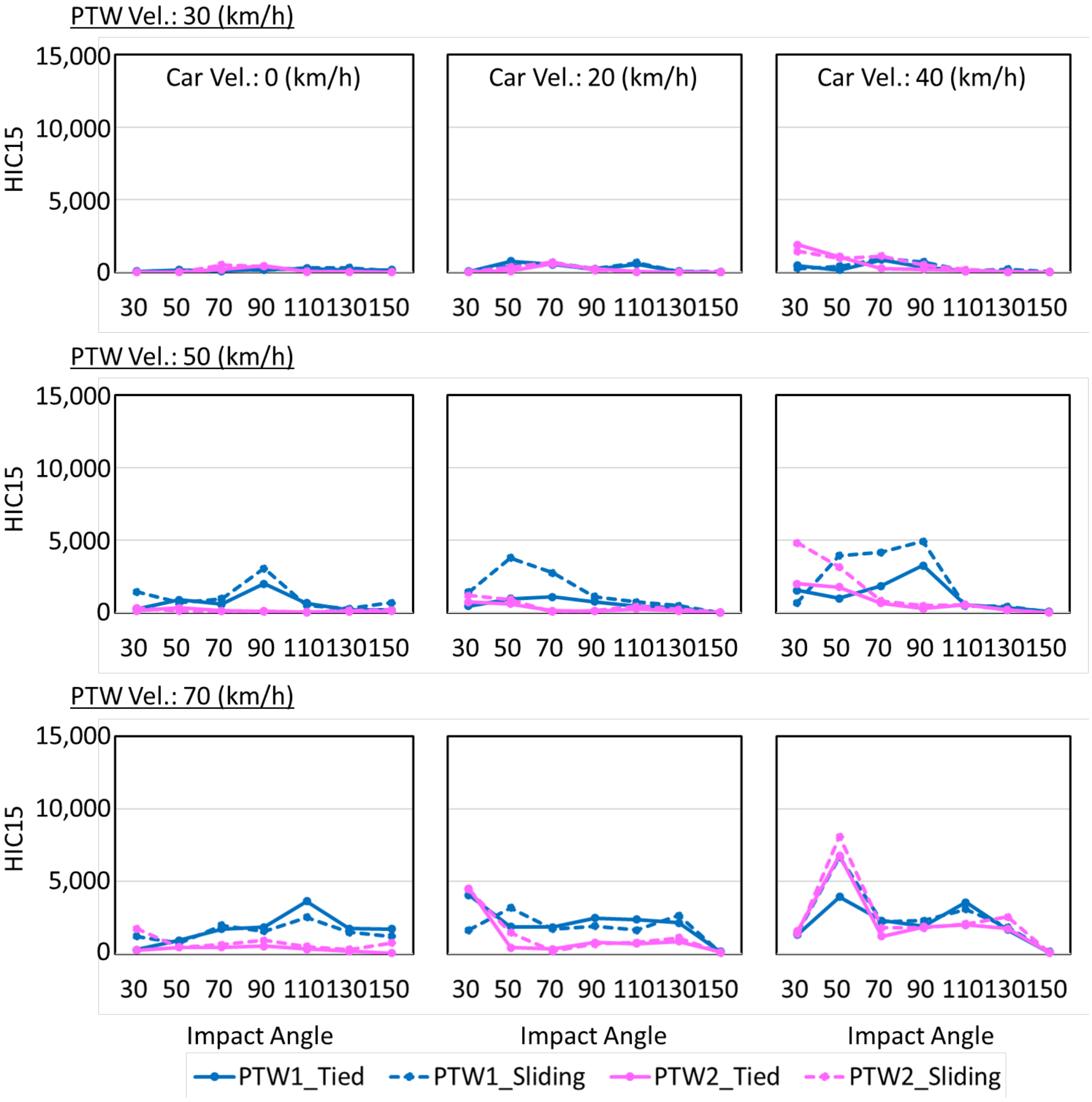

Fig. C1. Relationship between HIC15, and impact angle, car velocity and PTW velocity (A-pillar).

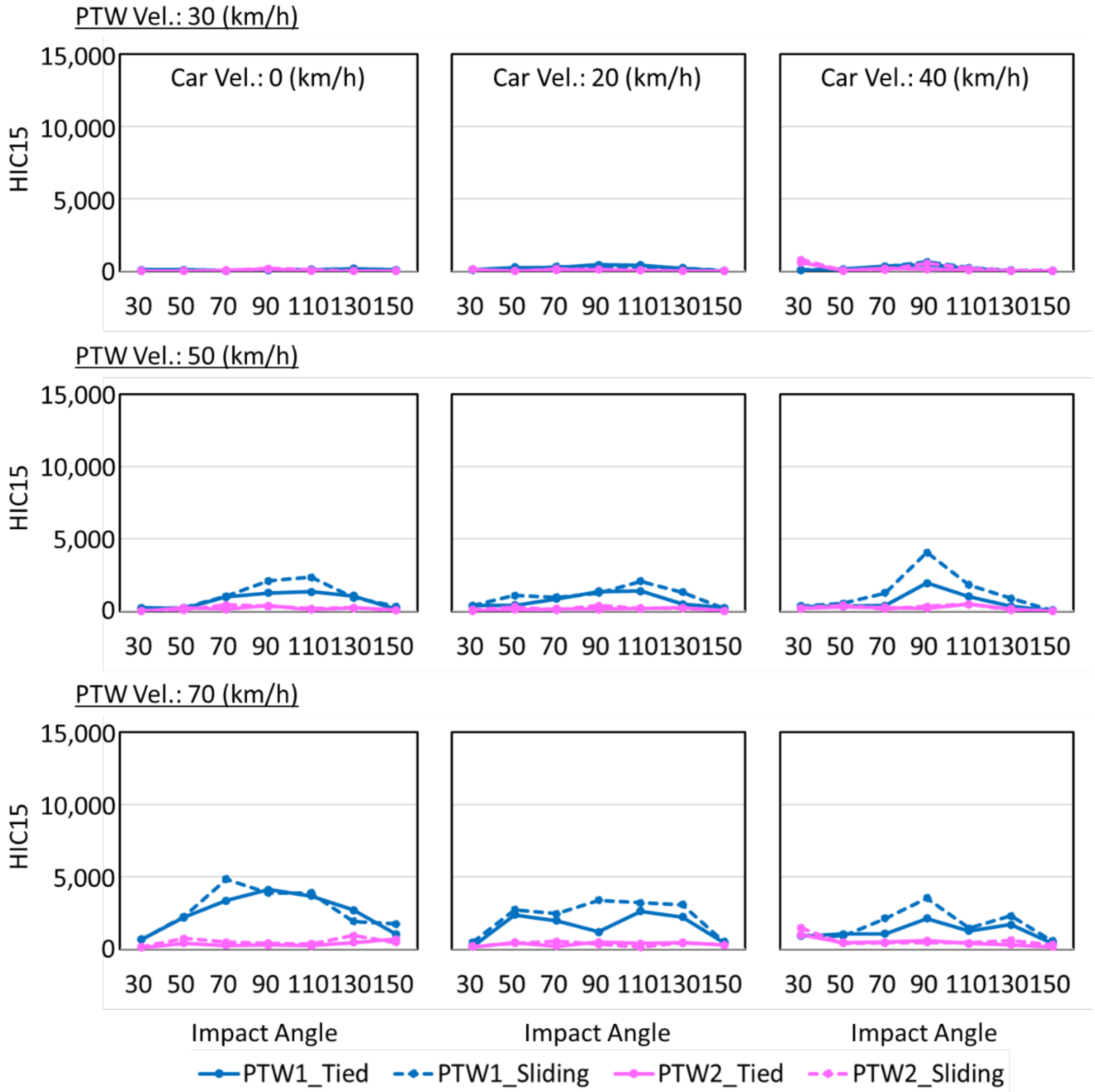

Fig. C2. Relationship between HIC15, and impact angle, car velocity and PTW velocity (B-pillar).

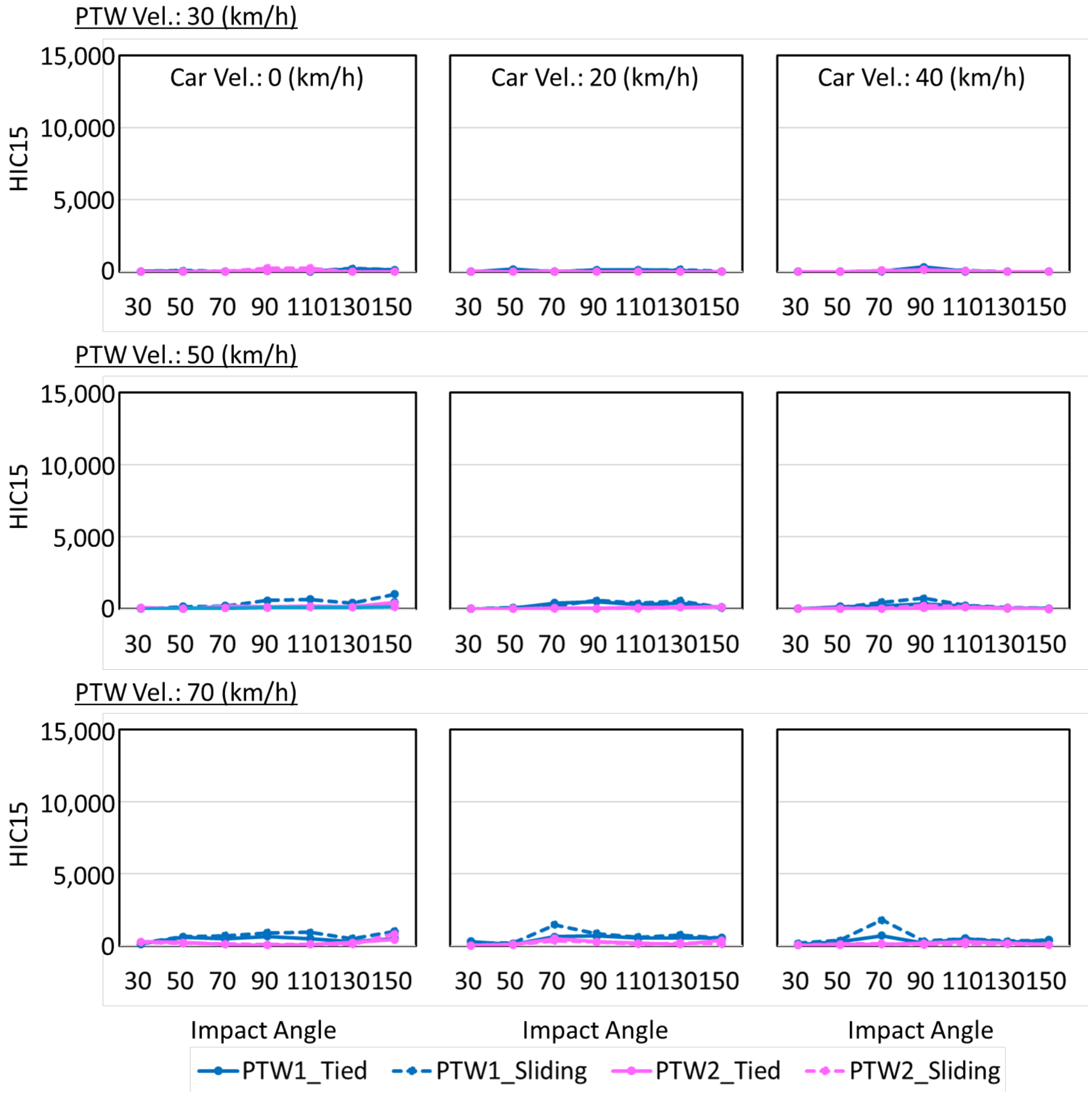

Fig. C3. Relationship between HIC15, and impact angle, car velocity and PTW velocity (C-pillar).

Appendix D: Influence of Impact Angle, Car Velocity and PTW Velocity (CAR3)

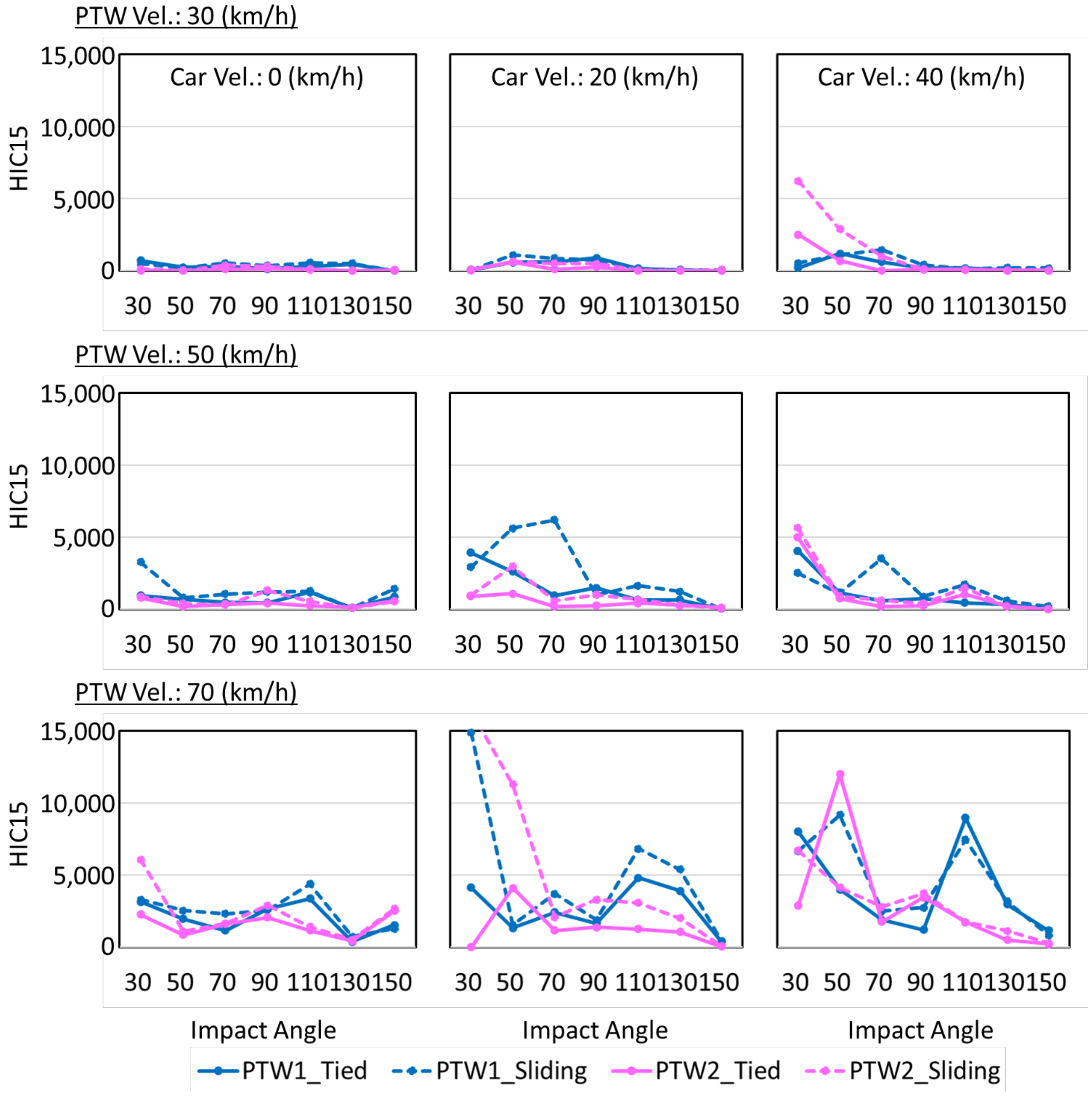

Fig. D1. Relationship between HIC15, and impact angle, car velocity and PTW velocity (A-pillar).

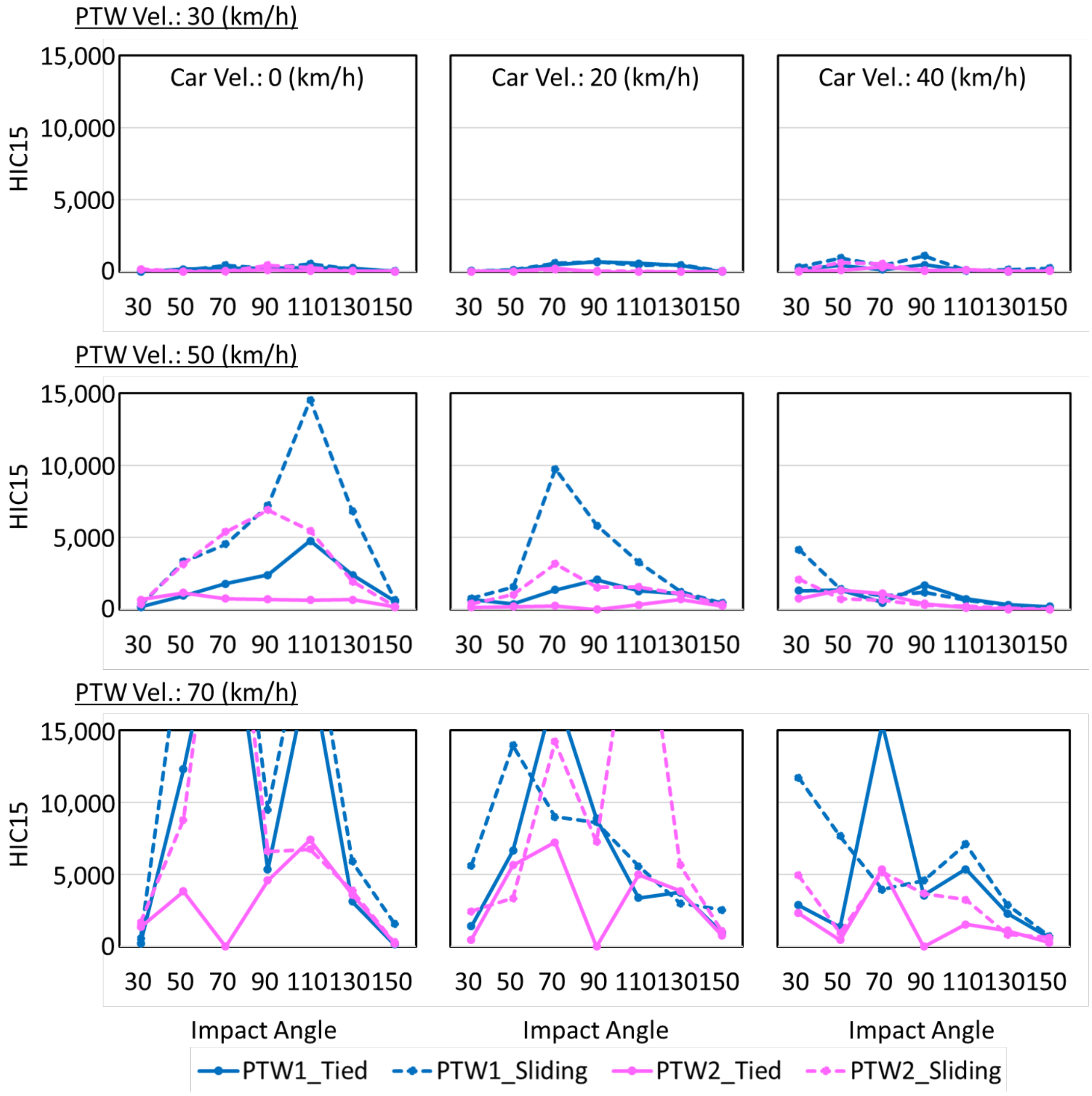

Fig. D2. Relationship between HIC15, and impact angle, car velocity and PTW velocity (B-pillar).

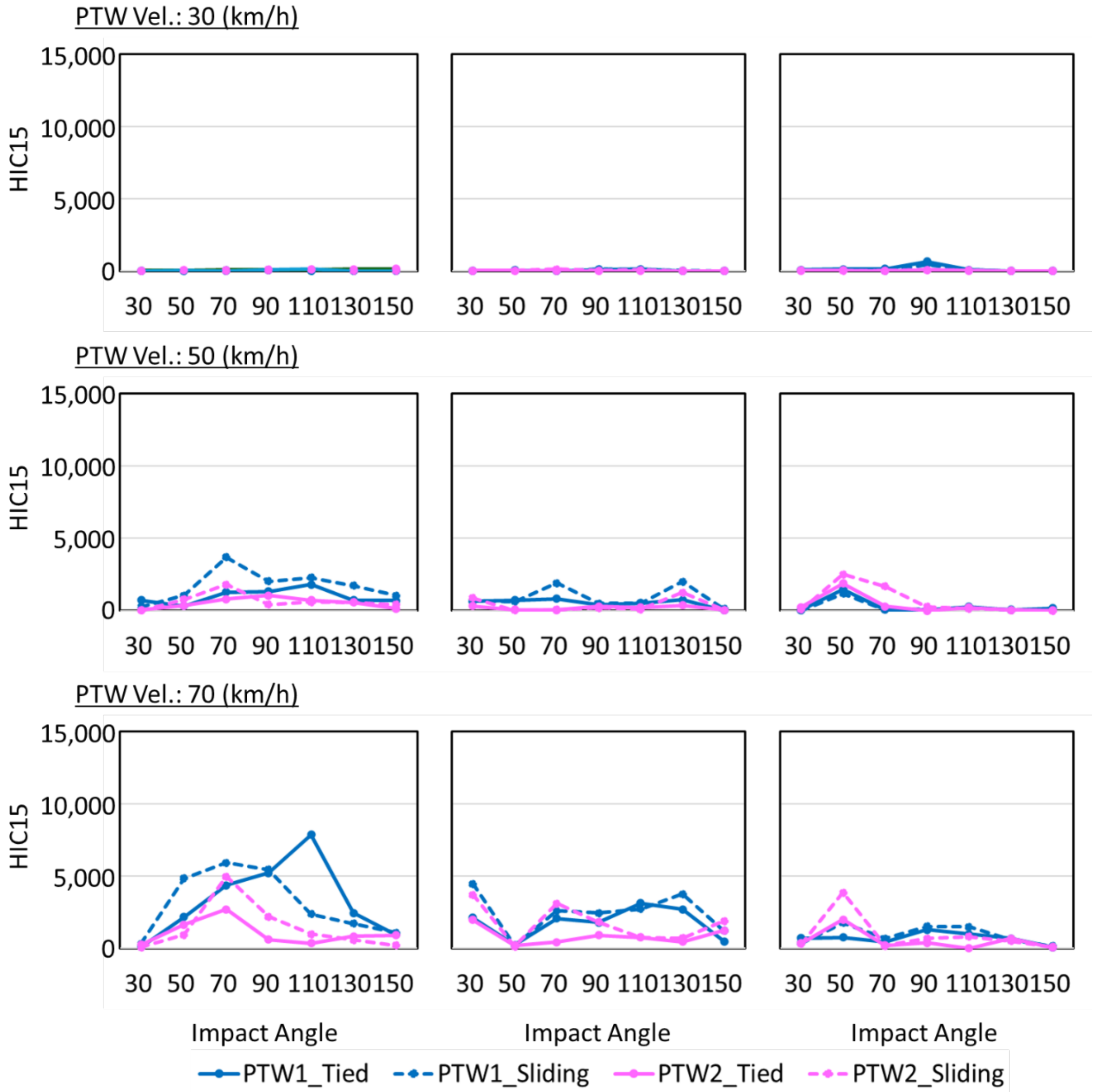

Fig. D3. Relationship between HIC15, and impact angle, car velocity and PTW velocity (C-pillar).

Appendix E: Influence of Impact Angle, Car Velocity and PTW Velocity (CAR4)

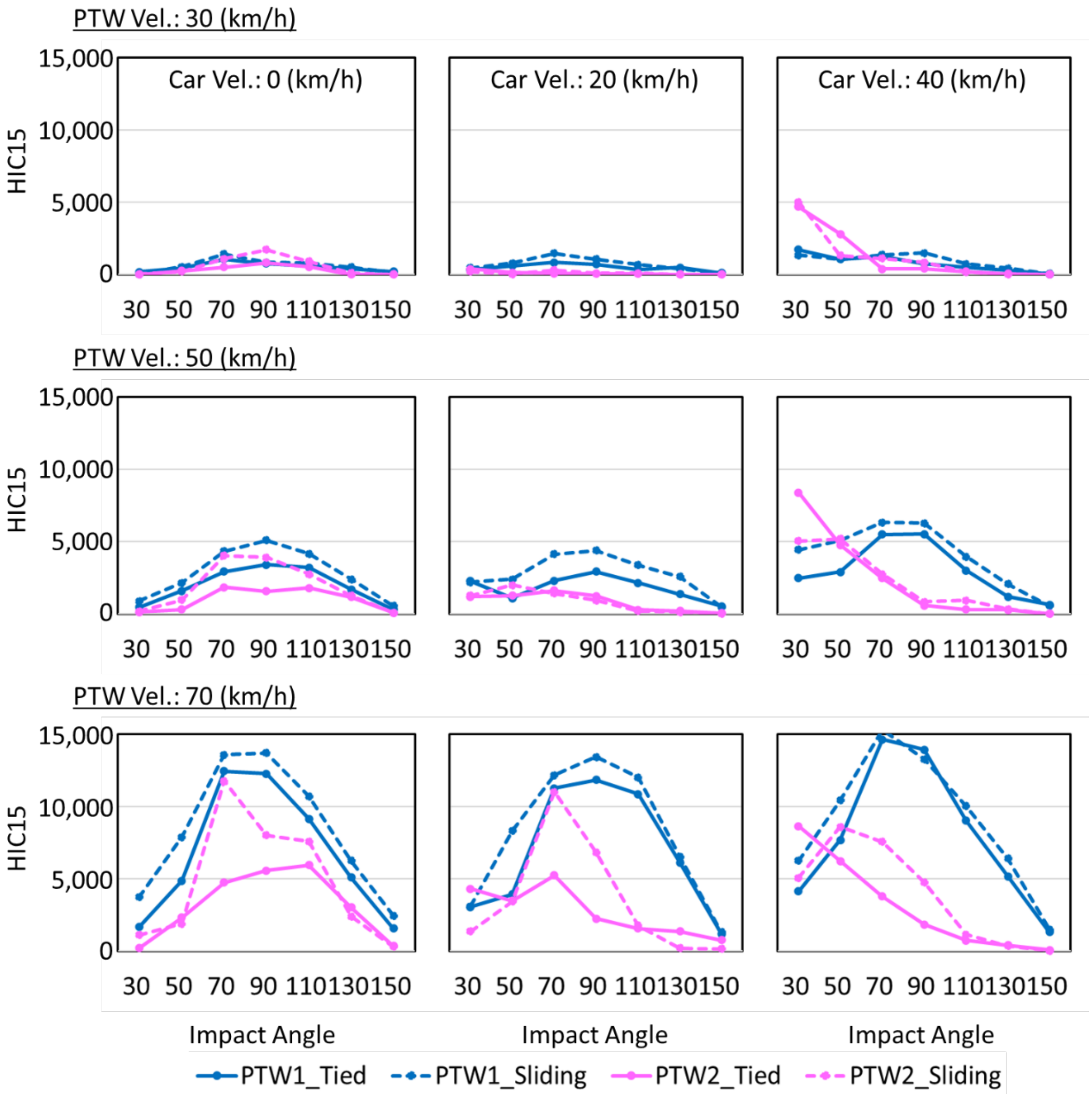

Fig. E1. Relationship between HIC15, and impact angle, car velocity and PTW velocity (A-pillar).

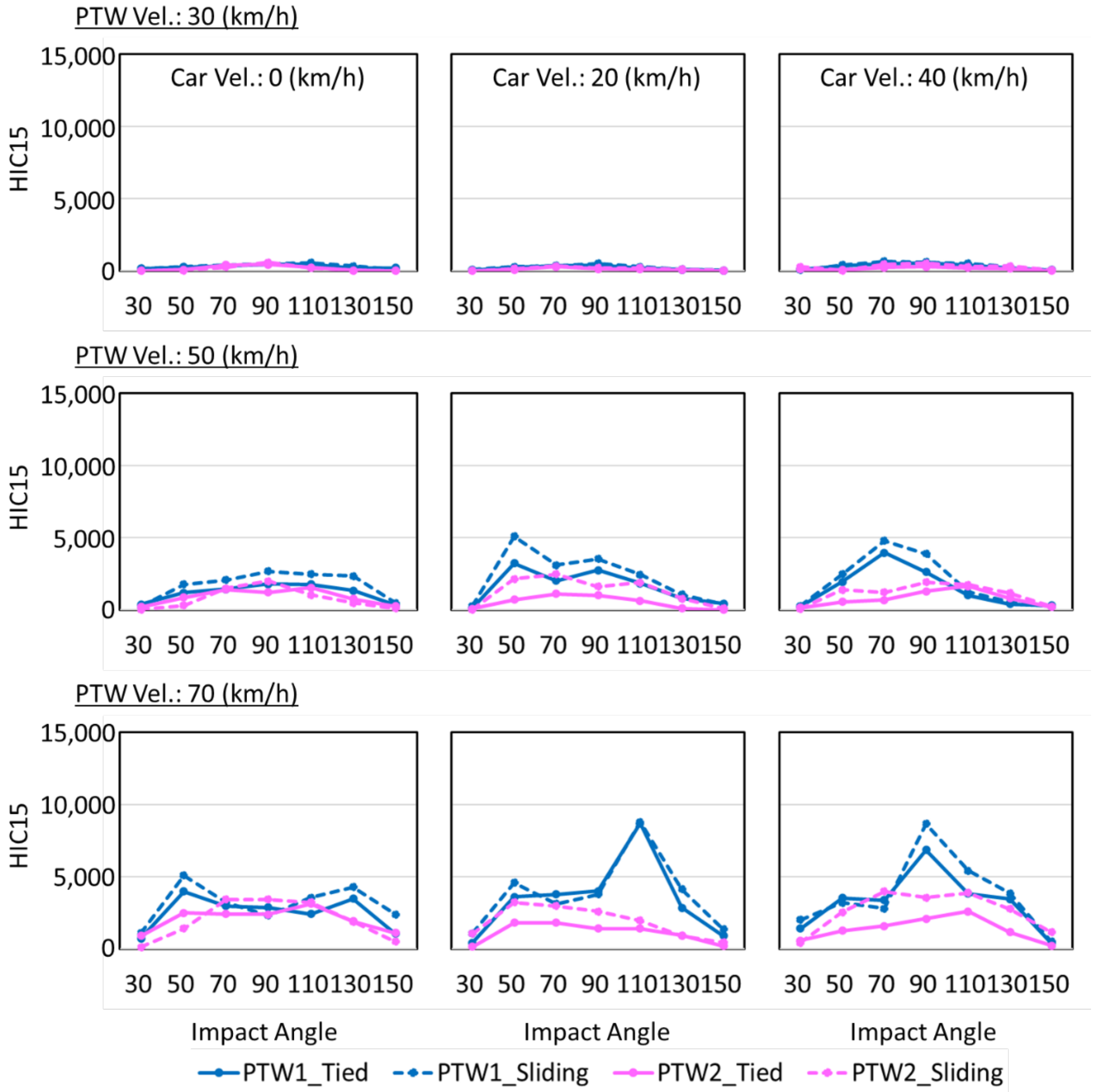

Fig. E2. Relationship between HIC15, and impact angle, car velocity and PTW velocity (B-pillar).

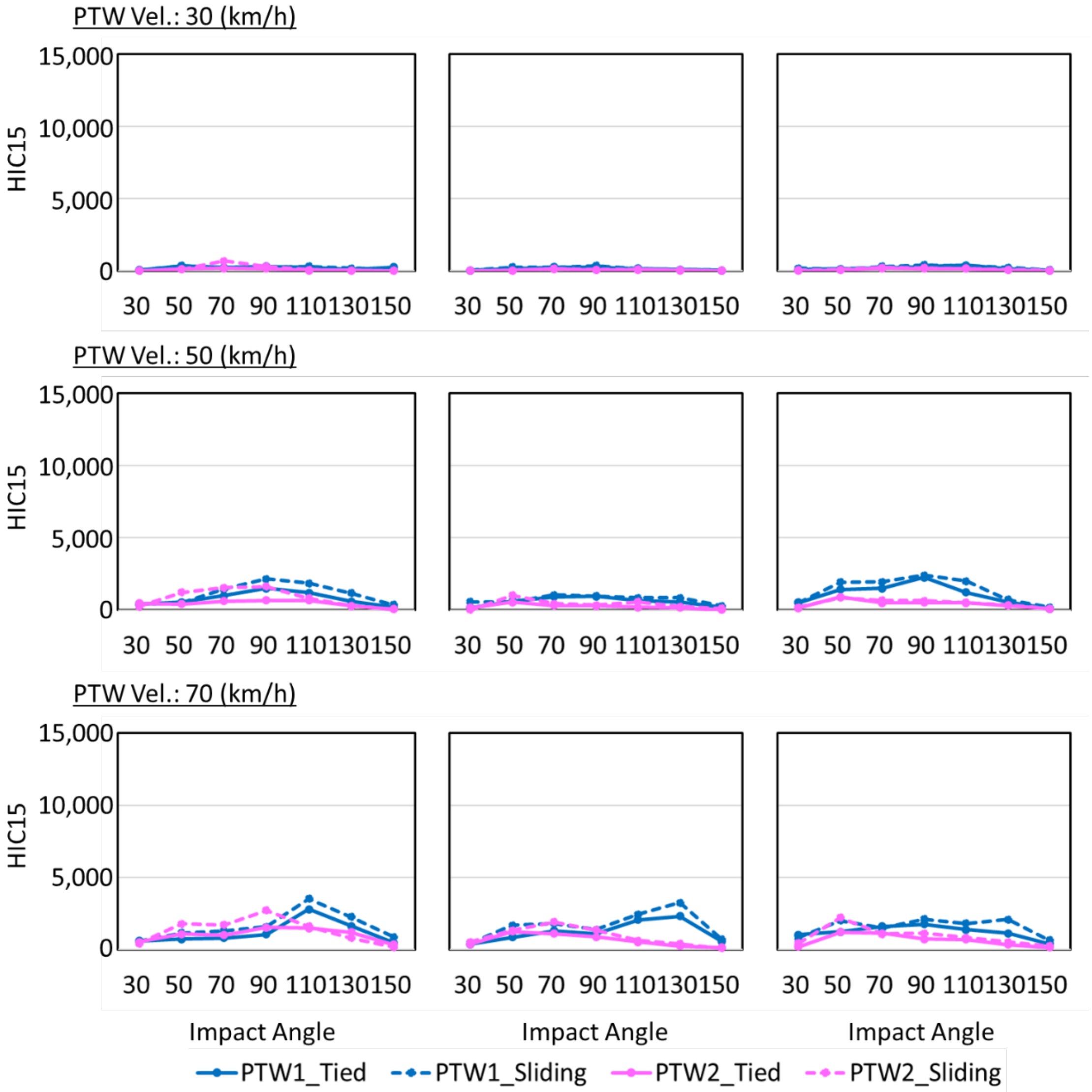

Fig. E3. Relationship between HIC15, and impact angle, car velocity and PTW velocity (C-pillar).

Appendix F: Influence of Impact Angle, Car Velocity and PTW Velocity (CAR5)

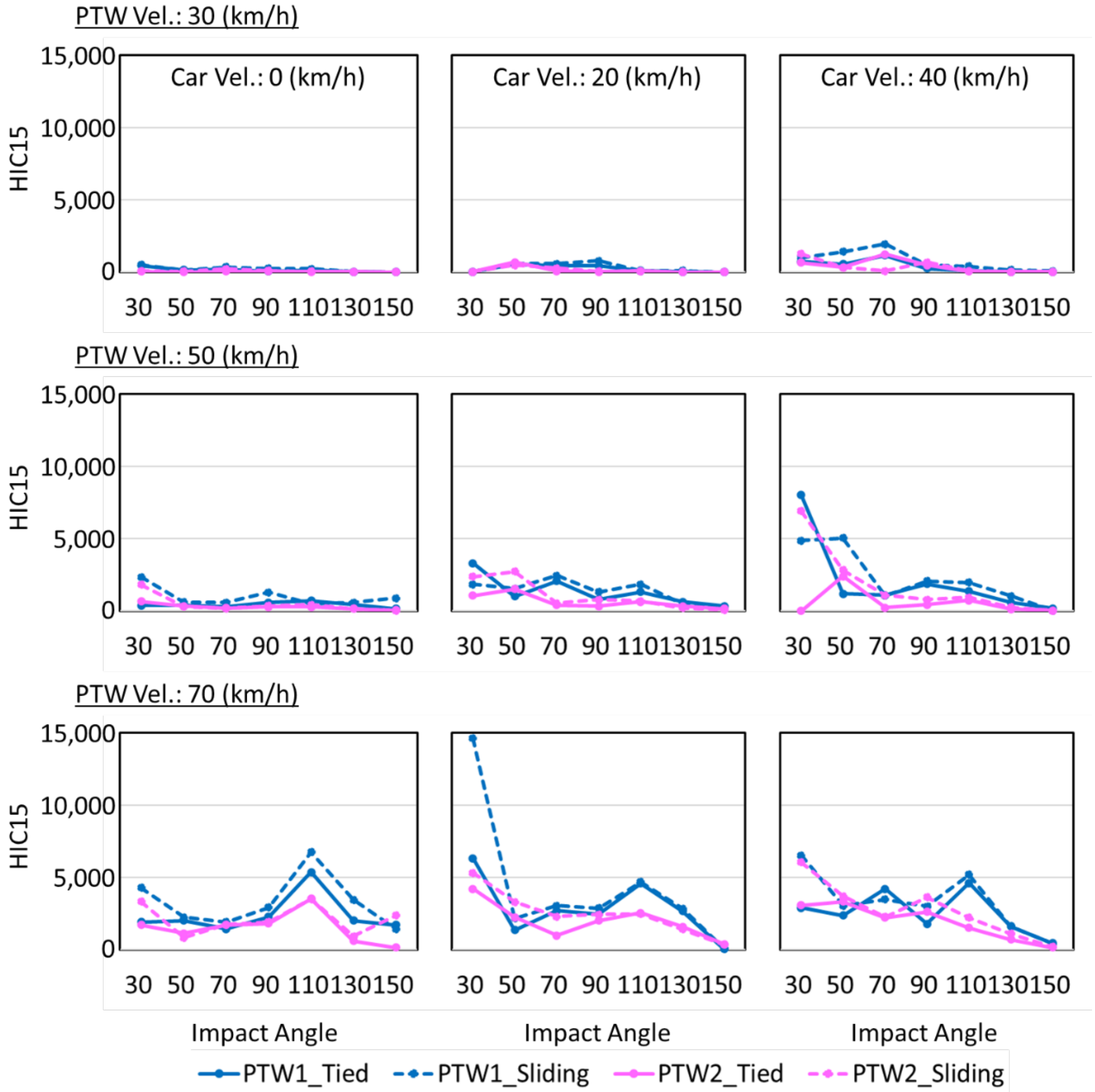

Fig. F1. Relationship between HIC15, and impact angle, car velocity and PTW velocity (A-pillar).

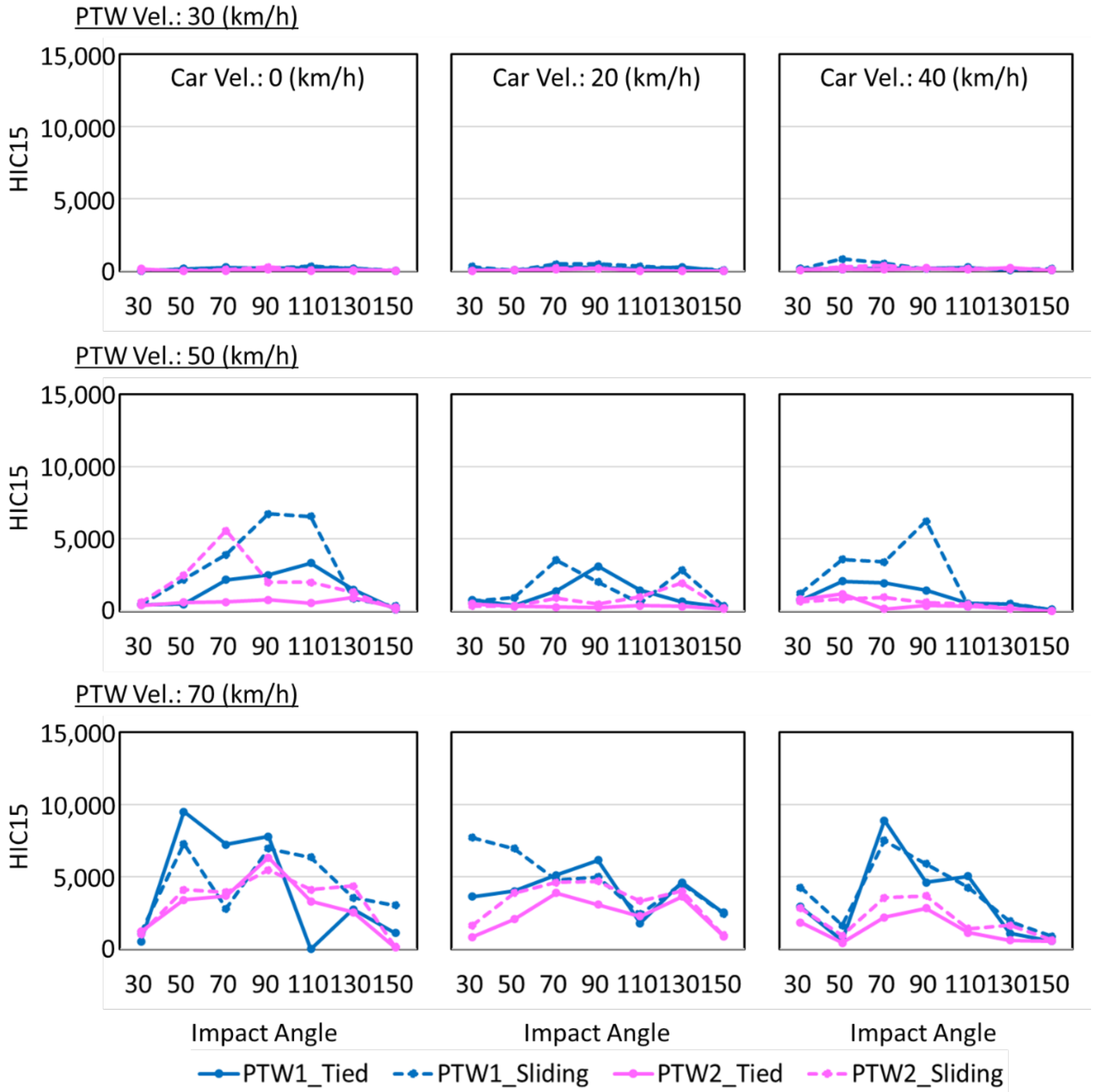

Fig. F2. Relationship between HIC15, and impact angle, car velocity and PTW velocity (B-pillar).

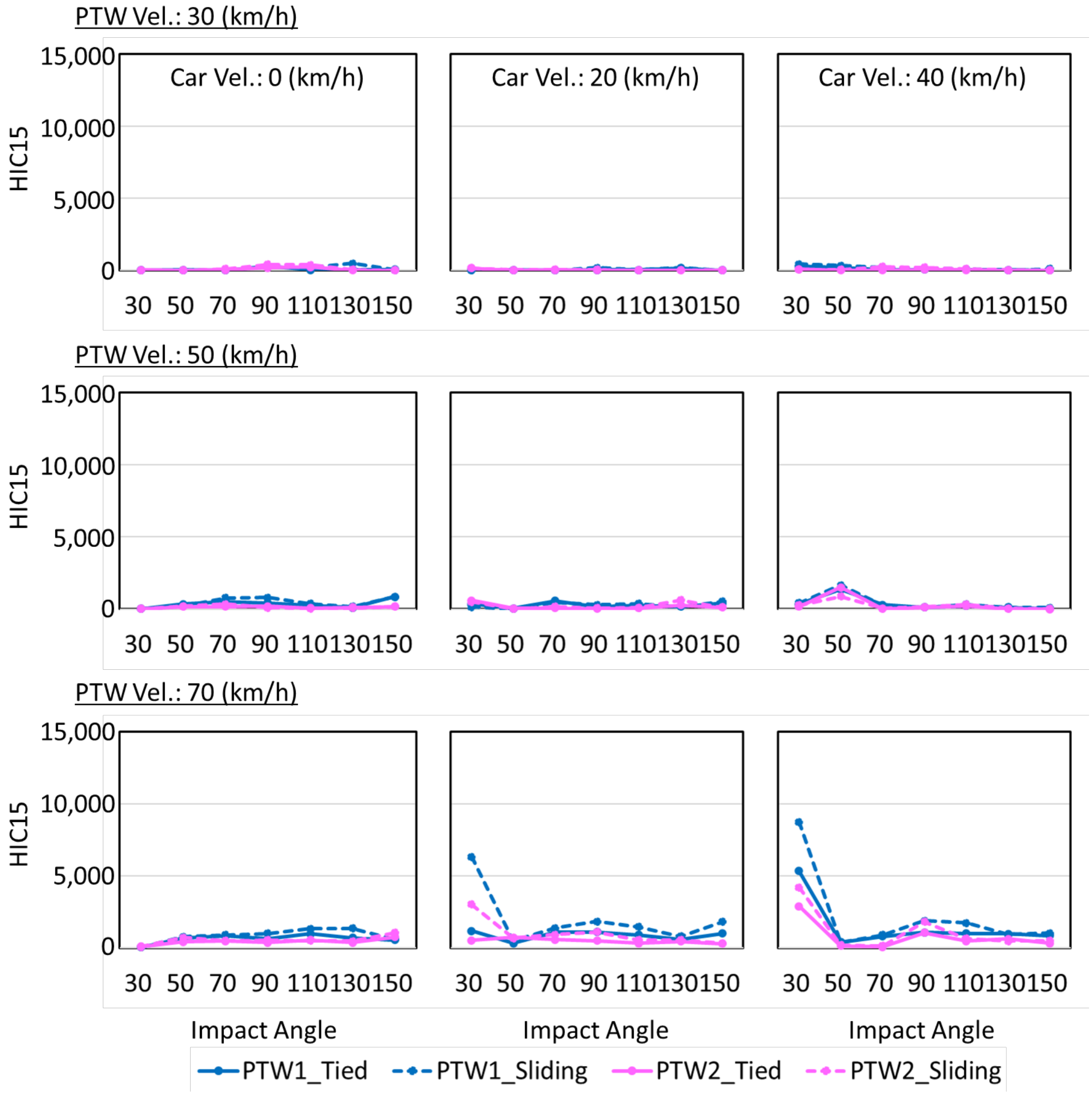

Fig. F3. Relationship between HIC15, and impact angle, car velocity and PTW velocity (C-pillar).

Appendix G: Influence of Impact Angle, Car Velocity and PTW Velocity (CAR6)

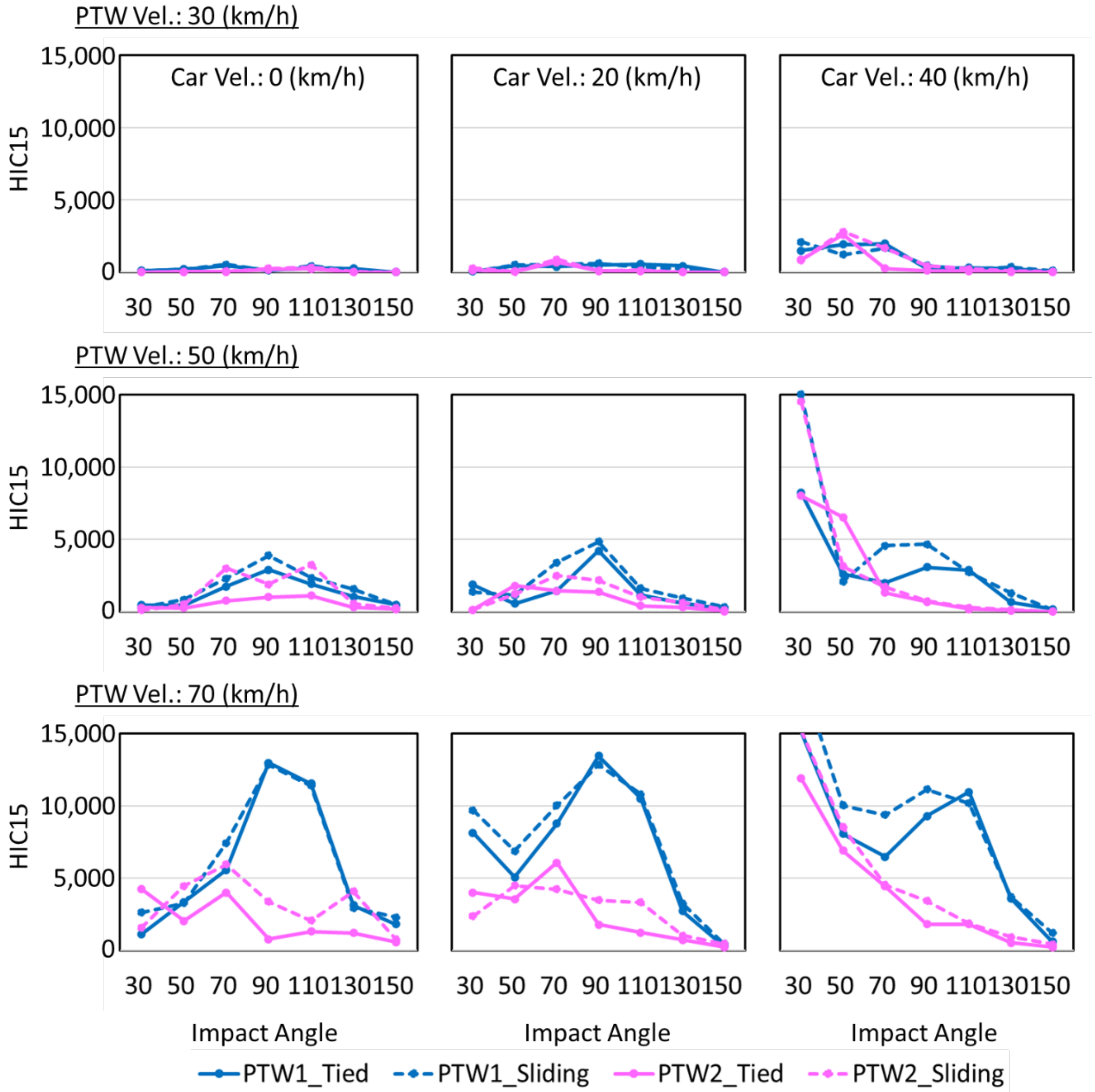

Fig. G1. Relationship between HIC15, and impact angle, car velocity and PTW velocity (A-pillar).

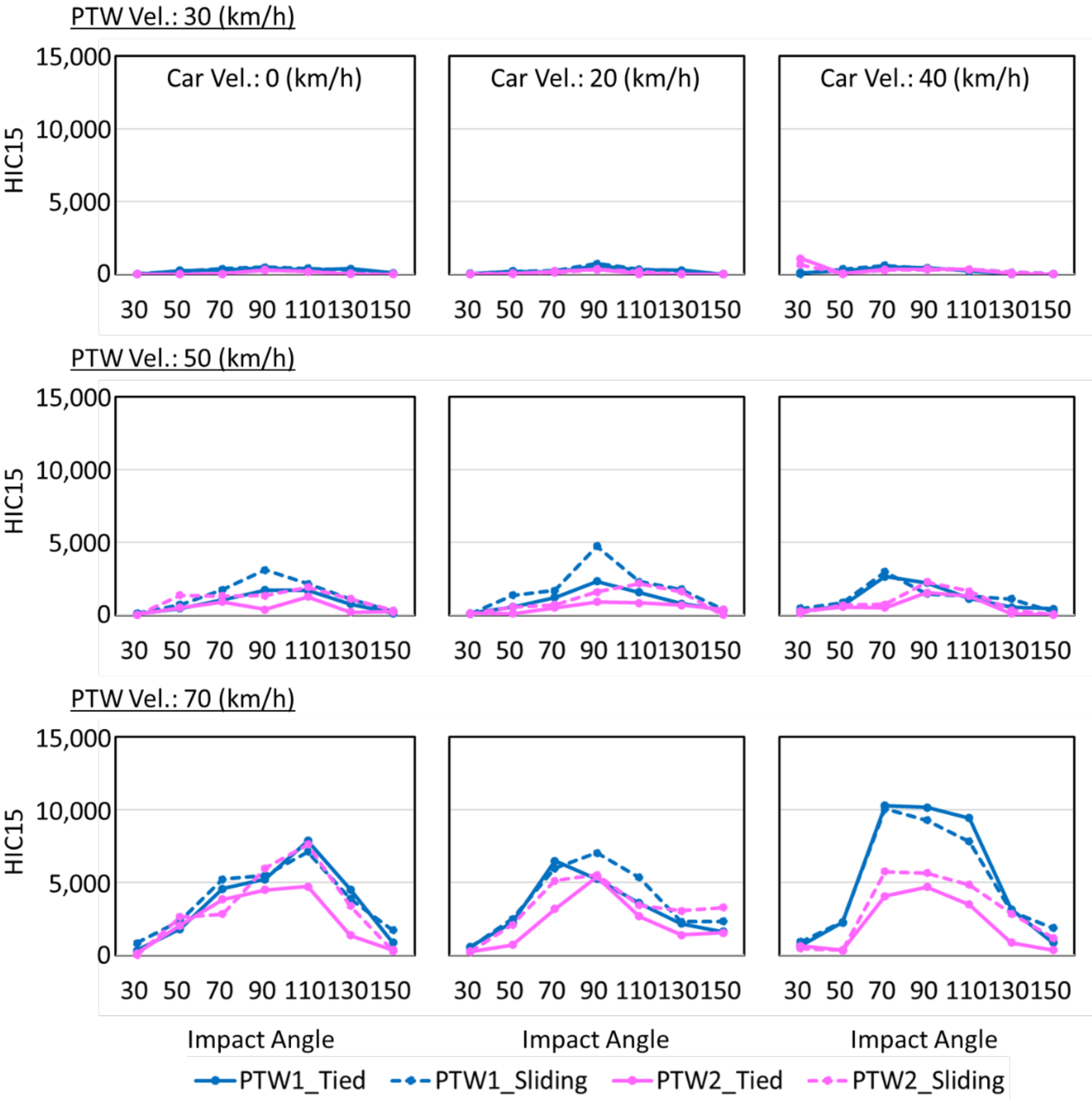

Fig. G2. Relationship between HIC15, and impact angle, car velocity and PTW velocity (B-pillar).

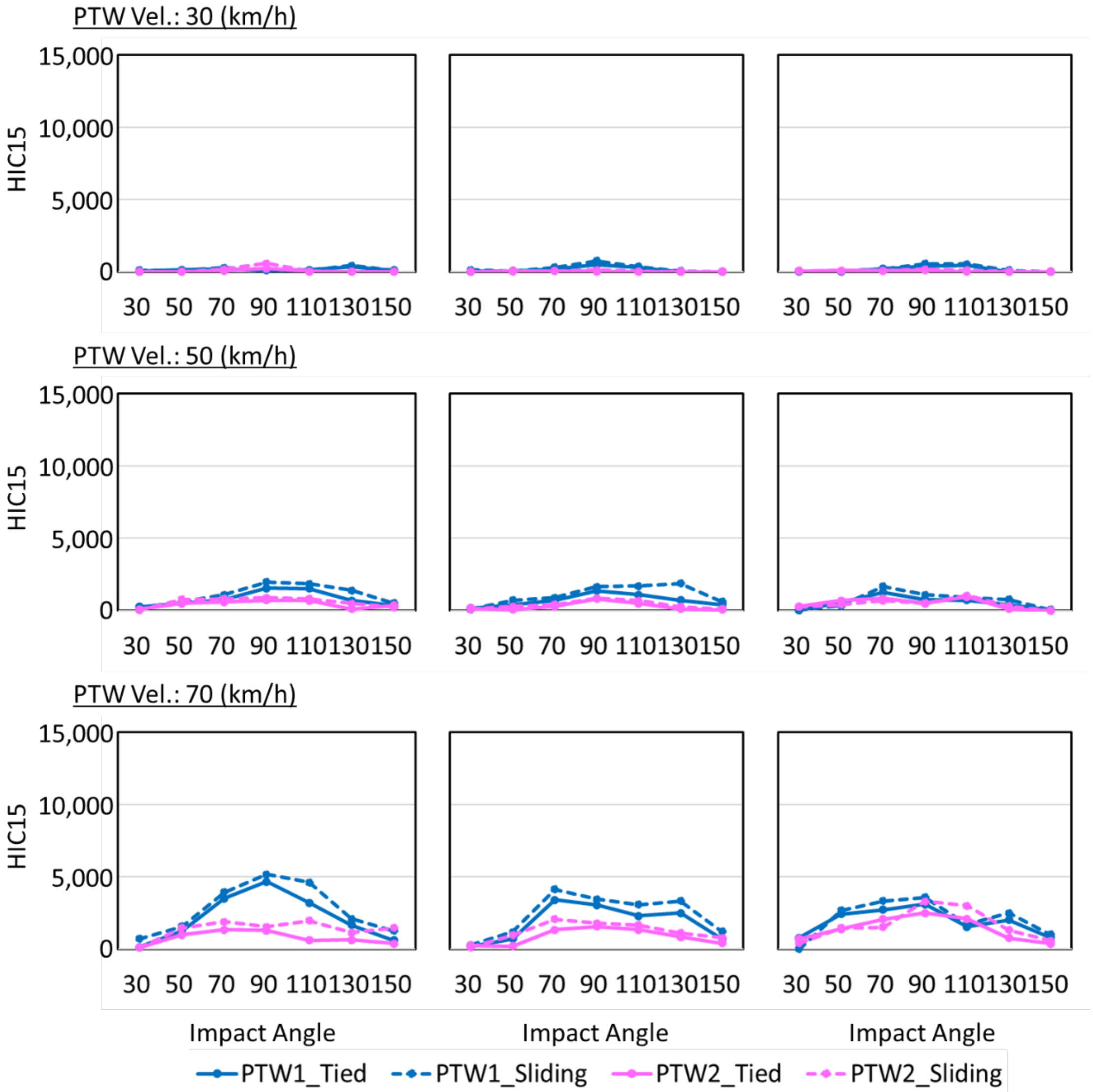

Fig. G3. Relationship between HIC15, and impact angle, car velocity and PTW velocity (C-pillar).